REGULATING INOSITOL BIOSYNTHESIS IN PLANTS: *MYO*-INOSITOL PHOSPHATE SYNTHASE AND *MYO*-INOSITOL MONOPHOSPHATASE

Jean Christine Styer

Thesis Submitted to the Faculty of
Virginia Polytechnic Institute and State University in
Partial Fulfillment of the Requirements for the Degree of

Master of Science

In

Biochemistry

Dr. Glenda E. Gillaspy, Chairperson

Dr. Elizabeth A. Grabau

Dr. John L. Hess

February 10, 2000
Blacksburg, Virginia

Keywords: *Myo*-inositol, *myo*-inositol-1L-phosphate synthase, inositol monophosphatase

REGULATING INOSITOL BIOSYNTHESIS IN PLANTS: *MYO*-INOSITOL PHOSPHATE SYNTHASE AND *MYO*-INOSITOL MONOPHOSPHATASE

Jean Christine Styer

ABSTRACT

Inositol is important for normal growth and development in plants. The regulation of the inositol biosynthetic enzymes, *myo*-inositol phosphate synthase (MIPS) and *myo*-inositol monophosphatase (IMP) was investigated. The specific aims of this research were (1) to develop a tool to study MIPS protein accumulation in a model plant system, *Arabidopsis thaliana* (*At*) and potentially other plant species and (2) to determine the spatial expression patterns of *Lycopersicon esculentum* IMP-2 (*Le*IMP-2) at the cellular level.

Myo-inositol phosphate synthase (mips) genes have been identified in plants, animals, fungi and bacteria. Alignment of the predicted amino acid sequences of *At*MIPS-1, -2 and *Glycine max* MIPS (*Gm*MIPS) indicated that *At*MIPS-1 and *Gm*MIPS are 87% identical, and *At*MIPS-2 and *Gm*MIPS are 89% identical. Based on these data, a *Gmmips* cDNA was fused at the N-terminus to a 6X histidine tag (5' GAC GAC GAC GAC GAC GAC 3'), cloned into an overexpression vector and overexpressed in *E. coli*. The fusion protein, HISMIPS, was extracted using denaturing conditions and purified using Ni^{2+} affinity chromatography. Anti-*Gm*MIPS antiserum from rabbit detected the recombinant HISMIPS protein (76 kD), and *Gm*MIPS (64 kD). Affinity purification by subtractive chromatography yielded anti-*Gm*MIPS antibody that detected *At*MIPS (66 kD) and a protein (34 kD) of unknown function. *At*MIPS accumulated to high levels in unopened flowers, opened flowers, and immature siliques (6 mm in length or less), but was not detectable in bolts, cauline or rosette leaves.

The tomato *inositol monophosphatase (Leimp)* genes are a developmentally regulated multigene family. From analysis of sequences, *Leimp*-2 is intron-less and has the putative start site of translation located at +108 bp downstream from the putative start site of transcription. Investigation of the 5' UTR revealed the 3' end of a partial open reading frame (338 bp) highly homologous to the gene for calmodulin. Three light responsive elements and a cold responsive element were also identified in the 5' UTR.

Transgenic *Leimp*-2::*uid*A plants were produced using the existing construct of the Le*imp*-2 promoter fused to the *uid*A gene (J. Keddie, University of California at Berkeley). Seedlings were perserved and sectioned. Using histological techniques, the analysis of the *Leimp*-2 promoter::*uid*A transgenic seedlings revealed that the *Leimp*-2 promoter causes expression at the base of the shoot apex and within leaflets of the first set of fully expanded leaves. Further, *Leimp*-2 promoter expression was localized to epidermal and cortex cells on the abaxial side of the 1st and 2nd fully expanded compound leaves.

These studies of MIPS and IMP expression lay a foundation for a better understanding of the regulation of inositol biosynthesis in Arabidopsis, tomato, and other plant species.

Table of Contents

List of Figures

List of Tables

PART I: LITERATURE REVIEW

THE IMPORTANCE OF INOSITOL

Myo-inositol (inositol) (Figure 1.1) is important for normal plant growth and development. The role of inositol in plants is many fold. Inositol participates in the phosphatidylinositol (PI) signaling pathway, auxin storage and transport, phytic acid biosynthesis, cell wall biosynthesis, and the production of stress related molecules (for reviews see Loewus and Murthy, 2000; Loweus, 1990) (Figure 1.2). Modification of inositol biosynthesis may offer potential solutions for practical agricultural problems.

Biotechnology tools, such as transgenic plant technology, are available for regulating inositol biosynthesis *in vivo*. However, to understand the importance of producing transgenic plants with modified inositol biosynthesis, it is first necessary to outline the many roles of inositol in the plant.

THE PI SIGNALING PATHWAY

Plants, like animals, require the ability to respond to their environment. Organisms utilize signal transduction cascades for the transport of information. Inositol is an essential component of one such signal transduction cascade in plants called the PI signaling pathway (for review see Munnik et al., 1998). The inositol produced from the PI signaling pathway can be added to intracellular inositol pools or recycled to the PI signaling pathway. This pathway has been shown to participate in a variety of plant responses including gravitrophism in *Zea mays* (Perera et al., 1999) and turgor pressure changes in stomatal guard cells (for review see Cote and Crain, 1993).

AUXIN STORAGE AND TRANSPORT

Plant hormones are potent facilitators of physiological change in plant tissues. Therefore, it is important for plants to provide a mechanism to transport hormones in a non-reactive form to target tissues or cells. Inositol has been hypothesized to play a central role in the control of the plant hormone auxin (indole acetic acid or IAA) (for review see Bandurski, 1980). Inositol conjugates of IAA are presently assumed to serve

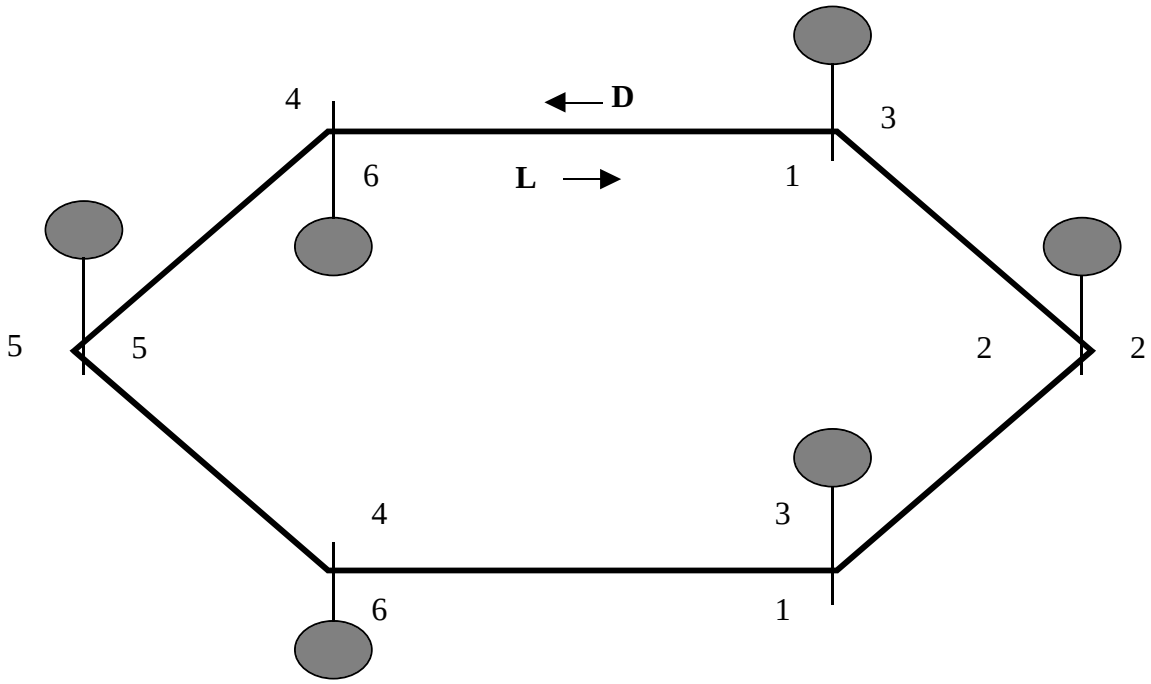

Figure 1.1 ***Myo*-inositol**. Inositol is a six-member carbon ring. Adapted from Loewus, (1990).

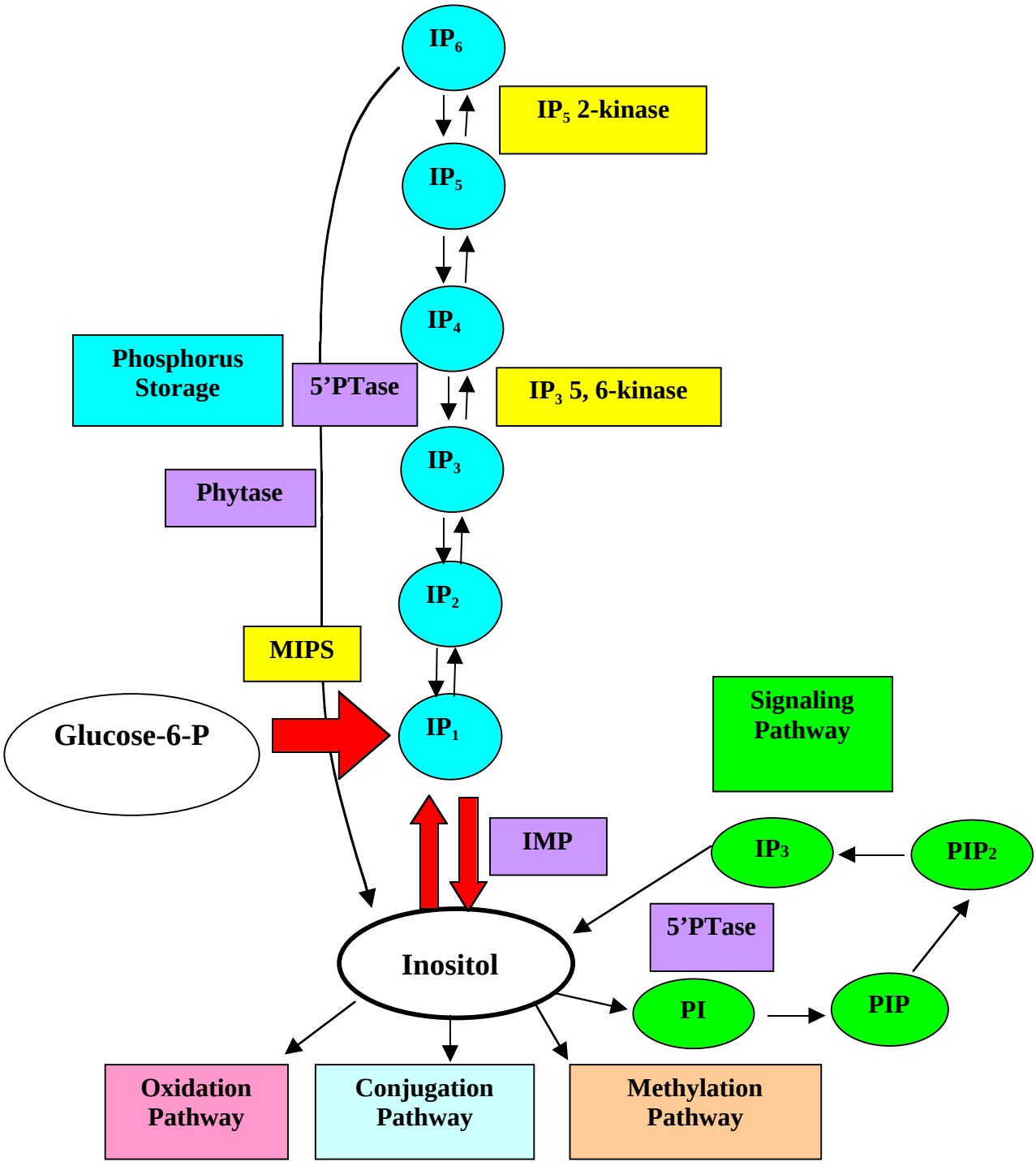

Figure 1.2 Inositol biosynthesis and utilization in plants. MIPS and IMP catalyze reactions in the *de novo* inositol biosynthesis pathway. Scavenged inositol phosphates from the phosphotidylinositol signaling pathway and IP_6 breakdown also provide inositol for intracellular pools.

as storage and/or transport of auxin and may regulate the availability of usable IAA for physiological responses. Maize enzymes capable of conjugating inositol to IAA have been isolated, as well as an esterase that may be involved in the catalysis of an auxin-inositol conjugate (Kowalczyk and Bandurski, 1991).

BIOSYNTHESIS OF PHYTIC ACID (IP_6)

Seeds store phosphorous as IP_6, a hexaphosphate ester of inositol (Loewus and Loewus, 1983). IP_6 molecules are deposited in the seeds in specialized cellular organelles called globoids. During seed germination, IP_6 is broken down into phosphorous and inositol by the enzyme phytase (for review see Loewus and Loewus, 1983).

IP_6 has been implicated in other roles such as seedling development. Shears (1996) suggests alternative roles for IP_6 such as inhibition of protein phosphatases, modulation of calcium channel activity, attenuation of endocytosis and inhibition of clathrin assembly. York et al. (1999) suggest that IP_6 plays a role in the nuclear pore complex and the nuclear transport of mRNA. In animals, IP_6 has been found to have anticancer effects in rats (Thompson, 1994) and antinutrient effects (Loewus and Loewus, 1983). The presence of indigestible IP_6 in animal diets has also lead to environmental phosphorous problems. Manipulation of IP_6 biosynthesis has been proposed to address some of these issues.

PLANT CELL WALL BIOSYNTHESIS

Inositol is also an essential molecule for the production of the plant cell wall. Most plants have both primary and secondary cell walls, the constituents of which are polysaccharides, proteins and lignin. Inositol is oxidized to form urosine diphosphate (UDP)-D-glucuronic acid. This oxidized inositol is the most common and important nucleotide sugar produced through the inositol oxidation pathway; it is both a precursor for other UDP-D-sugars (UDP-D-glucuronic acid, UDP-D-galacturonic acid, UDP-D-xylose, UDP-D-apiose and UDP-L-arabinose) and a donor for polysaccharide biosynthesis (Loewus and Murthy, 2000). In addition to cell wall biosynthesis, these

nucleotide sugars provide components for other pathways involved in transport, storage and development (Loewus and Loewus, 1983).

PRODUCTION OF STRESS RESPONSE-RELATED INOSITOL ISOFORMS

Inositol and the *o*-methyl inositols esters, D-ononitol (4-*o*-methyl inositol) and D-pinitol (1D-*o*-methyl-*chiro*-inositol), contribute to plant protection against salt stress (for review see Loewus and Murthy, 2000; Bohnert et al., 1995). The accumulation of inositol and inositol derivatives in response to salinity has been studied extensively in *Mesmbryanthemum crystallinum* (ice plant). Inositol, D-ononitol and D-pinitol are suggested to function in salt tolerance in two major ways: (1) to protect cellular structures from reactive oxygen species such as hydrogen peroxide, and (2) to control turgor pressure. Under salt stress conditions, the ice plant undergoes shock, and wilts for a short period of time, followed by synthesis and accumulation of inositol, D-ononitol and D-pinitol. After these osmolytic molecules accumulate, turgor pressure is restored and inositol is detected in the phloem (Nelson et al., 1998). Sodium (Na^+) and inositol accumulate in the leaves, suggesting that the mechanism for salt tolerance in ice plant involved controlling the proper direction of Na^+ transport (Nelson et al., 1998). Bohnert (1995) suggests that altering the biosynthesis of inositol and inositol derivatives may confer salt tolerance to crop species.

MANIPULATING INOSITOL BIOSYNTHESIS TO BENEFIT FARMERS

Developing control of inositol biosynthesis through biotechnology may yield products that afford the average American farmer with crop alternatives for problems related to salinity, environmental pollution by fertilizer, and the anti-nutrient properties of animal feed. Currently, salinity issues are being addressed using either complicated and extensive irrigation systems, or by finding agricultural relevance for naturally salt tolerant, halophytic, species (for review see Van-Schilfgaarde, 1993).

Addressing environmental pollution and anti-nutrition challenges can also be aided by regulating inositol biosynthesis. Soybean, a seed high in IP_6, is a common feed

for farm animals. The IP_6 an animal ingests through this type of grain-based diet cannot be broken down in the gut and is subsequently excreted in the animal's manure. A major cause of phosphorous pollution to waterways is the mismanagement of dairy, (Shirmohammadi et al., 1997), poultry and swine waste (Mallin et al., 1997). As a result, phosphorous accumulates in the environment causing disturbances in habitat homeostasis such as algal blooms and/or decreased stream water dissolved oxygen (Mallin et al., 1997).

Additionally, IP_6 is an anti-nutrient to farm animals. When passing through the gut IP_6 binds minerals, proteins and starch (for review see Thompson, 1994). Current approaches to mediating this problem include supplementing animal feed with a fungal phytase enzyme, or adding phosphorous to the animal feed; however, these methods are expensive for the average farmer (Bosch et al., 1998).

PRODUCTION OF INTRACELLULAR POOLS OF INOSITOL

Inositol participates in many different aspects of plant physiology. Two routes have been suggested for the production of intracellular inositol pools (1) the *de novo* biosynthesis and (2) the recycling of inositol phosphates. The *de novo* inositol biosynthesis pathway involves two enzymes: *myo*-inositol-1L-phosphate synthase (MIPS) (EC 5.5.1.4) and *myo*-inositol monophosphatase (IMP) (EC 3.1.3.25) (Loweus and Loweus, 1983). These two enzymes may interact with each other in an inositol biosynthesis metabolon, groups of enzymes producing inositol for a particular plant function. The first committed step in the *de novo* inositol biosynthesis pathway is the conversion of glucose-6-phosphate to 1D-inositol-3-phosphate by MIPS. Inositol is a negative feedback inhibitor of this conversion (for review see Majumder et al., 1997). Next, IMP catalyzes the dephosphorylation 1D-inositol-3-phosphate to produce inositol (for review see Parathasarathy et al., 1994). This is the only known *de novo* inositol biosynthesis pathway in plants (Loewus and Loewus, 1983).

Another route used to produce intracellular inositol pools is through the recycling or scavenging of inositol phosphates through the PI signaling pathway and IP_6 breakdown. The PI signaling pathway is stimulated by extracellular signals or ligands that bind transmembrane receptors. The receptor activates phospholipase C (PLC), which, in turn, cleaves phosphotidylinositol-4, 5 *bis*phosphate (PIP_2) into two second-messenger molecules, diacylglycerol and 1D-inositol-1, 4, 5-triphosphate (IP_3). IP_3 is released into the cytosol to interact with calcium-containing organelles. To break down IP_3, the cell sequentially dephosphorylates IP_3 to inositol phosphates. Inositol monophosphate, 1D-inositol-1-phosphate, is further dephosphorylated to inositol through a reaction that involves IMP. Therefore, IMP is required for both the *de novo* biosynthesis of inositol and the recycling of inositol through the PI pathway.

Plants can also scavenge inositol by the breakdown of IP_6. The dephosphorylation of IP_6 is catalyzed by phytase. There are two known types of phytase. One is primarily found in microorganisms, and the other is primarily found in plant seeds (Cosgrove, 1980). The plant phytase is a 6-phytase (*myo*-inositol hexakisphosphate-6-phosphohydrolase, E.C. 3.1.3.26). This enzyme hydrolyzes IP_6 into inositol and free phosphate.

mips AND imp GENES

Mips and *imp* genes have been isolated in plants, animals, and microorganisms. By using sequence data, it is possible to develop strategies for isolating these genes from other species and to determine evolutionary relationships. Organisms from which *mips* genes have been sequenced include: *Brassica napus* (*Bnmips*) (Hussain et al., 1997), Arabidopsis (*Atmips*-1; Johnson, 1994), (*Atmips*-2; Johnson and Burk, 1995), soybean (*Gmmips*) (Hegeman et al., unpublished data), *Hordeum vulgare* (*Hvmips*) (Larson and Raboy, 1998), *Mesmbryanthemum crystallinum* (ice plant) (*Mcmips*) (Ishitani et al., 1996), *Nicotiana panciulta* (*Npmips*) (Hashimoto et al., 1999), *Oryza sativa* (rice) (*Osmips*) (Yoshida, 1999), *Sacchromycecs cerevisiae* (yeast) (*Scmips*) (Johnson and Henry, 1989), *Spirodela polyrrhiza* (*Spmips*) (Smart and Fleming, 1993), *Triticum*

aestivum (*Tamips*) (Hussain, 1999) and *Zea mays* (*Zmmips*) (Larson and Raboy, 1998). Accession numbers can be found in Table 1.1.

Imp has been cloned and sequenced from only a few plant species. A detailed picture of plant IMP, in particular in relation to functionality, has been provided in *Lycopersicon esculentum* (tomato). There are three *imp* genes in tomato, *Leimp*-1, -2 and -3 (Gillaspy et al., 1995). Other plants from which *imp* has been sequenced include *Gossypium hirsutum* (cotton) (*Ghimp*) (Blewitt et al., 1999), Arabidopsis (*Atimp*) (Gillaspy, unpublished data) and *Mesmbryanthemum crystallinum* (*Mtimp*) (Nelson and Bohnert, 1997). Accession numbers can be found in Table 1.1.

Mips and *imp* are members of multigene families in some plant species. Arabidopsis *mips* (*Atmips*) consists of *Atmips*-1 (Johnson, 1994) and *Atmips*-2 (Johnson and Burk, 1995) and possibly *Atmips*-3 (Ishitani et al., 1996). Accession numbers can be found in Table 1.1. *Atmips*-1 and -2 encode proteins with predicted molecular weights of 56.21 kD and 56.1 kD respectively; however, *Atmips*-3 is an incomplete cDNA and further analyses need to be completed to determine if this is a true isoform of *At*MIPS. In the crop species *Zea mays* (corn) and soybean, the *mips* gene family is estimated to contain at least seven and four gene family members, respectively (Larson and Raboy, 1999; Grabau et al., unpublished data). *Mcmips* may also belong to a multigene family in the ice plant as suggested by low-stringency DNA blots (Ishitani et al., 1996).

Plant *imp*s are also a part of a multigene family. *Leimp*-1, -2 and -3 encode proteins with apparent molecular masses of 30, 29 and 28 kD, respectively (Gillaspy et al., 1995). The Arabidopsis *imp* (*Atimp*-3) has also been isolated, sequenced and found to exhibit phosphatase activity *in vitro* (Gillaspy et al., unpublished data). The protein has a molecular weight of 28 kD. Preliminary protein blot analysis suggests other *At*IMP isoforms exist which correspond in size to those found in tomato.

Table 1.1 Accession numbers for *mips* and *imp* genes. Sequences can be accessed through GenBank.

Enzyme	Accession Number	Source	No. Amino Acids	Predicted Molecular Mass[a]	References
MIPS	AAC07613[b]	*Aquifex aeolicus*	364	40.7	Deckert et al., 1998
MIPS	U04876	*Arabidopsis thaliana-1*	511	56.5	Johnson, 1994
MIPS	AL022605	*Arabidopsis thaliana-2*	510	56.3	Johnson and Burk, 1995
MIPS	U66307	*Brassica napus*	509	56.2	Hussain et al., 1997
MIPS	NA	*Glycine max*	511	56.5	Hegeman et al., unpublished data
MIPS	AF056325	*Hordeum vulgaris*	510	56.2	Larson and Raboy, 1998
MIPS	U32511	*Mesembryanthemum crystallinum*	512	56.8	Ishitani et al., 1996
MIPS	AAB85594[b]	*Methanobacterium thermoautotrophicum*	361	40.8	Smith et al., 1997
MIPS	AB032073	*Nicotiana paniculata*	510	56.4	Hashimoto et al., 1999
MIPS	AB012107	*Oryza sativa*	510	56.2	Yoshida et al., 1999
MIPS	X87371	*Sacchromyces cerevisiae*	537	61.2	Johnson et al., 1989
MIPS	S60302	*Spirodela polyrrhiza*	510	56.4	Smart and Fleming, 1993
MIPS	CAB38887[bc]	*Streptomyces coelicolor*	361	39.9	Redenbach et al., 1998
MIPS	AF120146	*Triticum aestivum*	510	56.3	Hussain, 1999
MIPS	AF56326	*Zea mays*	510	56.2	Larson and Raboy, 1998
IMP	ATT2268[b]	*Arabidopsis thaliana*	286	31.6	Gillaspy et al., unpublished
IMP	AW187977	*Gossypium hirsutum*	209	22.8	Blewitt et al., 1999
IMP	U39444	*Lycopersicon esculentum-1*	273	30.0	Gillaspy et al., 1995
IMP	U39443	*Lycopersicon esculentum-2*	268	29.5	Gillaspy et al., 1995
IMP	U39059	*Lycopersicon esculentum-3*	265	29.1	Gillaspy et al., 1995
IMP	AF037220	*Mesembryanthemum crystallinum*	270	29.2	Nelson and Bohnert, 1997

[a] Molecular masses calculated using EditSeq (Lasergene Software, DNAstar)

[b] Sequences can be accessed through GenPept

[c] Putative gene

TEMPORAL AND SPATIAL REGULATION OF MIPS

A temporal and spatial component to regulation of inositol biosynthesis by MIPS and IMP exists in plants. MIPS transcripts and/or proteins are (1) developmentally regulated (Yoshida et al., 1999; Johnson and Wang, 1996; Hegeman et al., unpublished), (2) localized to chloroplasts (Johnson and Wang, 1996), (3) up-regulated in response to salt water stress (Ishitani et al., 1996; Nelson et al., 1998) and abcissic acid (ABA) (Smart and Fleming, 1993) and (3) down regulated in response to non-photosynthetic conditions (Keller et al., 1999; Nelson et al., 1998). However, data describing MIPS protein expression patterns are limited in the literature, probably due to a lack of cross-reacting anti-MIPS antiserum.

Spatial and temporal regulation of MIPS comes as no surprise when considering inositol participation in signal transduction and IP_6 biosynthesis. MIPS has been localized at the level of transcription to immature tissues of rice (Yoshida et al., 1999) and soybean (Hegeman et al., unpublished data), and at the protein level in *Phaseolus vulgaris* (green bean) (Johnson and Wang, 1996). In rice, *Osmips* transcript accumulates to high levels in the embryos, but not in shoots, roots and flowers (Yoshida et al., 1999). Detailed analysis of rice embryos using RNA *in situ* hybridization indicate *Osmips* expression is localized to the globular stage of the embryo. Interestingly, *Osmips* transcript co-localizes with the formation of the protein bodies that contain IP_6 (Yoshida et al., 1999).

Soybean seed differentially expresses *mips* transcript (Hegeman et al., unpublished data). Immature soybean seeds contain higher levels of *Gmmips* transcript than mature soybean seed, leaves and roots, which contain low levels of *Gmmips* transcript (Hegeman et al., unpublished data). MIPS is also differentially expressed in the green bean (Johnson and Wang, 1996). Two putative *Pv*MIPS proteins were detected, apparent molecular weights 56 and 33 kD, using anti-*Sc*MIPS antiserum. The 56 and 33 kD putative *Pv*MIPS proteins were localized by protein blotting to specific

stages of embryo development where the suspensor and cotyledon develop (Johnson and Wang, 1996). Protein blot analysis also indicates the 33 kD protein is expressed in the roots and chloroplasts.

The spatial regulation of MIPS not only involves specific tissue types but also localization to plastids versus the cytosol. In addition to the 33 kD chloroplastic *Pv*MIPS (Johnson and Wang, 1996), chloroplastic isoforms of MIPS have been reported from rice, *Vigna radiata* (mung bean), *Euglena gracilis* and *Spirulina platensis* (cyanobacteria) with apparent molecular masses of 60 kD, 66.5 kD, 62 kD and 58 kD respectively (RayChaudhuri et al., 1997). It is intriguing that the 33 kD *Pv*MIPS putative chloroplastic protein is similar in size to bacterial MIPS from *Methanobacterium thermoautotrophicum* (40.8 kD) (Smith et al., 1997), *Aquifex aeolicus* (40.7 kD) (Deckert et al., 1998) and *Streptomyces coelicolor* (39.9 kD) (Redenbach, et al., 1998) (Accession numbers can be found in Table 1.1).

Spatial and temporal expression of MIPS transcript and protein occurs in the ice plant in response to salt stress and in the aquatic plant, *Spirodela polyrrhiza*, in response to the plant hormone ABA. The halophytic ice plant was found to upregulate *Mcmips* mRNA in response to salt-water treatment (Ishitani et al., 1996). Maximum levels of *Mcmips* transcript were detected after two hours of salt-water treatment and remained at this level until five days after salt-water treatment. Interestingly, identical experiments using the glycophytic plant Arabidopsis did not indicate increased levels of *Atmips* transcript. In fact, *Atmips* transcript remained constant regardless of the salt-water treatment applied (Ishitani et al., 1996).

Salt stress conditions elicit specific spatial expression patterns of *Mc*MIPS protein (Nelson et al., 1998). During normal non-salt-stressed conditions, *Mc*MIPS protein was present at low levels and was localized to the phloem and sieve elements. After salt-water treatment, *Mc*MIPS protein expression reached maximum levels within 24 hours in the leaves. In the roots, however, salt-water treatment caused *Mc*MIPS proteins to accumulate to levels less than before salt-water treatment (Nelson et al., 1998).

Immunocytochemistry targeted the increase in *Mc*MIPS to the mesophyll cells surrounding the phloem cells (Nelson et al., 1998). Analysis of the phloem exudate from salt-water stressed ice plants indicated increases in inositol and the inositol derivative D-onoitol. These experiments support the involvement of MIPS in a mechanism that confers salt tolerance in the ice plant (Nelson et al., 1998).

The plant hormone ABA affects specific tissue types and cells in the formation of the turion in *S. polyrrhiza*. Smart and Fleming (1993) isolated *Spmips* and found that the transcript of this gene is spatially and temporally regulated in the stolon. The stolon is a plant tissue that connects the dormant bud, or turion, to the mature plant. *Spmips* transcript is upregulated 30 minutes after ABA treatment and reaches maximum expression levels at 90 minutes post-ABA treatment.

Finally, studies of *mips* transcription in plants have indicated light/dark regulation. In *Solanum tuberosum* (potato), Keller et al. (1998) found *Stmips* is expressed at higher levels in photosynthetic tissues such as mature leaves, immature leaves, green flower buds, and colored flower buds than in non-photosynthetic tissue such as roots. Additionally, *mips* transcript accumulation decreases when light grown potato leaves are placed in dark conditions (Keller et al., 1998). Similarly, diurnal fluctuation of *Mcmips* protein was noted during normal light/dark changes (Nelson et al., 1998).

TEMPORAL AND SPATIAL REGULATION OF IMP

IMP is spatially and temporally regulated at the mRNA and protein levels. Comprehensive studies of IMP transcript and protein have been performed in tomato (Gillaspy et al., 1995), and Arabidopsis IMPs (*At*IMP) are currently being explored (Gillaspy, unpublished data). RNAse protection assays were used to determine transcript expression in various tomato tissues. *Leimp*-1 and -3 mRNA were easily detectable in most tomato seedling organs. In contrast, *Leimp*-2 transcript is ten-fold less abundant than either *Leimp*-1 or -3. *Leimp*-1 mRNA is most highly expressed in flowers, young and mature green fruit, light grown seedlings and callus; *Leimp*-2 transcript accumulation

is highest in seedlings, roots, and young fruit; *Leimp*-3 transcript was detected at high levels in the shoot apex and callus and at lower levels in the root, stem, leaf, flower, and young and mature green fruit. These results indicate *Leimp* transcript expression is highly regulated by developmental cues in tissues with established inositol requirements.

Although *Leimp*-2 transcripts were rare, investigation of *Le*IMP-2 protein levels indicated the protein was abundant. Anti-*Le*IMP-1 antiserum was produced, affinity purified and found to cross-react with the three isoforms of *Le*IMP. The three plant proteins correlated with the predicted sizes of each *Le*IMP gene product. Protein blot analysis of different tomato developmental stages indicated *Le*IMP proteins accumulate in callus, light grown seedlings, roots, leaves, young fruit, 1-cm diameter fruit and mature green fruit. Moreover, *Le*IMP-2 protein accumulated to a higher degree than *Le*IMP-1 or -3 as evident in callus, young fruit, 1-cm fruit and mature green fruit. The low level of transcript coupled with readily detectable *Le*IMP-2 protein, indicated *Le*IMP-2 may be expressed at high levels in specific cell types. This result also suggested post-transcriptional regulation of *Le*IMP-2. Immunocytochemistry analysis revealed *Le*IMP protein expression is localized to vascular tissue (Gillaspy et al., 1995). Nevertheless, the anti-*Le*IMP-1 antiserum readily detects all three isoforms, making it necessary to differentiate the cellular spatial expression patterns of these three isoforms by other means.

Preliminary analysis indicated that at least one *At*IMP isoform exists in this model plant system (Gillaspy et al., unpublished data). Using the anti-*Le*IMP-1 antiserum, total protein extracts from various Arabidopsis tissues were analyzed and a protein of 28 kD was detected. The size of the putative *At*IMP protein correlated with the apparent size of *Le*IMP-3 (Gillaspy, unpublished data). *At*IMP was most abundant in the siliques (Arabidopsis fruit bodies), flowers and etiolated seedlings. Stems, leaves and whole seedlings accumulated very low levels of *At*IMP protein. Interestingly, in etiolated seedlings, two proteins were noted, which may suggest a second *At*IMP isoform.

OBJECTIVES

The long-term objective of this work is to regulate the biosynthesis of inositol through genetic engineering. Manipulation of inositol availability in plants is possible through the alteration of the two enzymes involved in the inositol biosynthesis pathway, MIPS and IMP. However, before developing transgenic plants, basic research involving the two biosynthetic enzymes is necessary.

Unaddressed issues in the understanding of inositol biosynthesis enzymes include (1) the regulation of *At*MIPS isoforms at the protein level and (2) the spatial expression patterns of *Le*IMP-2 at the cellular level. Although *mips* mRNA and protein expression have been documented in some plants, a comprehensive study of all MIPS isoforms has not been performed in a single species. An anti-MIPS antiserum could be an important tool for analyzing MIPS protein accumulation for such a study. The plant model system Arabidopsis, with a short regeneration time, ease of transformation and nearly sequenced genome, allows for the rapid analysis of biological and biochemical processes. Production of an antiserum that cross reacts with Arabidopsis and potentially other plant species would provide a means for a detailed analysis of MIPS protein accumulation in plants.

Leimp is a multigene family in tomato (Gillaspy et al., 1995). Individual *Le*IMP proteins are differentially expressed and localized to specific tissues in tomato seedlings. However, the anti-*Le*IMP-1 antiserum cross-reacts with all three isoforms and as a result the specific spatial expression patterns of *Le*IMP-2 protein at the cellular level have not been elucidated. Localizing *Leimp*-2 at the level of transcription is also difficult since the transcript is rare. Analysis of the *Le*IMP-2 promoter region and promoter expression studies may provide a means to analyze the regulation of the *Le*IMP-2 isoform.

Therefore, the specific objectives of this research are:

Regulating Inositol Biosynthesis in Plants: *Myo*-Inositol Phosphate Synthase:

To develop an antiserum to detect MIPS isoforms and analyze MIPS protein accumulation patterns in the model system Arabidopsis and other plant species.

Regulating Inositol Biosynthesis in Plants: *Myo*-Inositol Monophosphatase.

To determine spatial expression patterns of *Le*IMP-2 at the cellular level.

PART II: REGULATING INOSITOL BIOSYNTHESIS IN PLANTS: *MYO*-INOSITOL PHOSPHATE SYNTHASE

INTRODUCTION

Inositol plays many important roles in the normal growth and development of plants, understanding the biosynthesis of inositol has become an important area of research. This six-member carbon ring is involved in signal transduction, phytic acid biosynthesis, osmoprotection, auxin storage and transport, and plant cell wall biosynthesis (for review see Loewus and Murthy, 2000).

Considerable progress has been made in understanding the role of the first committed enzyme in inositol biosynthesis, MIPS (for reviews see Loewus and Murthy, 2000; Majumder et al., 1997; Loewus, 1990). MIPS has been found to be regulated in response to developmental cues (Yoshida et al., 1999; Hegeman et al., unpublished data; Johnson and Wang, 1996) and salt-water stress (Ishitani et al., 1996; Nelson et al., 1998). In rice, *mips* transcript is upregulated and localized to modified organelles that contain phytic acid (Yoshida et al., 1999). Hegeman et al. (unpublished data) also indicate that high levels of *mips* transcript coincide with the accumulation of high levels of phytic acid in immature soybean seeds. Additionally, MIPS is developmentally regulated in the embryos of the *Phaseolus vulgaris* (green bean), in particular during the development of the cotyledon and the suspensor (Johnson and Wang, 1996). Upregulation of *mips* in response to salt water stress also revealed a role for inositol as an osmoprotectant. Salt water stressed *Mesembryanthemum crystallinum* (ice plant) accumulated high levels of *mips* transcript (Ishitani et al., 1996). Ice plants with elevated levels of MIPS also have increased levels of inositol in the phloem exudate (Nelson et al., 1998).

Through the use of transgenic plant technology, it may be possible to modify inositol biosynthesis. In order to prove that a transgenic phenotype is due to the altered expression of *mips*, it is essential to characterize MIPS protein levels. A tool for detection of MIPS protein would be the production of an anti-MIPS antiserum. Previously, anti-MIPS antiserum was raised against *Sacchromyecs cerevisiae* MIPS (*Sc*MIPS) (Johnson and Henry, 1989), *Euglena gracilis* MIPS (*Eg*MIPS) (RayChaudhuri et al., 1997) and ice plant MIPS (*Mc*MIPS) (Nelson et al., 1998). However, these anti-MIPS antisera have limited usefulness to our present studies in that they are either not

readily available or are not expected to cross react with MIPS proteins from higher dicots.

In this thesis, I have raised an anti-*Gm*MIPS antiserum against a soybean seed recombinant MIPS protein for the detection of MIPS proteins in Arabidopsis and potentially other agriculturally important species. *Gm*MIPS and *At*MIPS-1 and –2 are highly identical. *At*MIPS-1 and *Gm*MIPS are 86% identical, and *At*MIPS-2 and *Gm*MIPS are 89% identical. Therefore, it was highly likely an antiserum raised against *Gm*MIPS would cross react with *At*MIPS-1 and -2. This antiserum was found to immuno-react with the recombinant protein (HISMIPS), and MIPS proteins from Arabidopsis and soybean. The antiserum cross-reacts with both *At*MIPS-1 and –2, which suggests that it may be more sensitive than the anti-*Sc*MIPS antiserum previously used to detect *At*MIPS protein accumulation (Johnson and Sussex, 1995).

MATERIALS AND METHODS

PLASMIDS, BACTERIA STRAINS AND PLANT MATERIALS

The following plasmids and bacterial strains were used: pEThisMIPS and pLYSs (Novagen) (provided by C. Hegeman and E. Grabau, Virginia Polytechnic Institute and State University), pPOLYHIS*NIFU* and BL 21 (DE 3) (provided by D. Dean, Virginia Polytechnic Institute and State University) and pBluescriptSK(+) (SK) (Stratagene). *Arabidopsis thaliana* (Arabidopsis) ecotype Columbia was used in all experiments.

PLANT GROWTH CONDITIONS

Arabidopsis wild type seeds were sterilized in 30% v/v bleach for ten minutes and rinsed three times with sterile deionized/distilled water. Sterilized seeds were resuspended in 0.1% sterile agarose and plated on Murashige-Skoog Basal Salts Mixture (MS-Salts) (Sigma) under growth conditions of 24^{o}C and 16-hour light cycles. Plates were checked daily for plant seed germination. After three to four weeks, seedlings were transferred to soil and maintained under a humidity dome until bolts appeared. At this time, the dome was removed. Seedlings were maintained at 22^{o}C and watered from the bottom. Tissues were collected and stored at –80^{o}C.

INDUCTION AND EXTRACTION OF HISMIPS FUSION PROTEINS

A seed-specific soybean *(Glycine max* [L.] Merr. cv. Williams 82) *Gmmips* gene was isolated and sequenced. A partial-length *Gmmips* cDNA of 1425 basepairs (bp) (478 amino acids) was sub-cloned into a pET-32a (+) vector forming pEThisMIPS. The plasmid was transformed into *Escherichia coli* (*E.coli*) cell strain BL21 (DE3) pLYSs (Novagen). The predicted size of the recombinant protein produced by this construct is 70 kD. The portion of *Gmmips* cDNA in the fusion construct encodes for 52 kD of the recombinant protein. The remaining 18 kD of fusion protein consists of a N-terminal 6X-histidine tag, a thiroredoxin tag and an S-tag (Novagen). Construction of pEThisMIPS was performed by C. Hegeman (Virginia Polytechnic Institute and State University).

The HISMIPS recombinant protein was overexpressed using protocols provided by the Qiagen Expressionist handbook (Qiagen). One bacterial colony containing the pEThisMIPS construct was inoculated into 50 ml of Luria Bertani (LB) broth with 34 μg/ml of chloroamphenicol and 50 μg/ml of ampicillin, and incubated for 12 hours at 37^{o}C at 175 revolutions per minute (rpm). The overnight culture was diluted 1:20 in LB broth with the above antibiotics. The culture was grown to an optical density at 600 nm (OD_{600}) of 0.6 as determined by a spectrophotometer (Beckman DU 640B). At this time, isopropyl β-D-thiogalactopyranoside (IPTG) was added to the culture to a final concentration of 1 mM. After ten hours at room temperature (22-24^{o}C) (RT) the culture was centrifuged at 4000 rpm for 20 minutes at 4^{o}C (Eppendorf Centrifuge 5810R). The supernatant was decanted and the cell pellets were stored at –20^{o}C.

The fusion protein was extracted using both non-denaturing and denaturing conditions as outlined by the Qiagen Expressionist Handbook. The cell pellets were resuspended in either non-denaturing lysis buffer (5 mM imidazole, 0.5 M NaCl and 20 mM Tris-HCl pH 7.9), or denaturing lysis buffer (8 M Urea, 0.1 M sodium phosphate buffer, and 0.01 M Tris-HCl pH 8.0) at 5 ml of buffer per 1 gram of cell pellet. Lysates were rocked at RT for 1 hour and quick-frozen at -80^{o}C for 15 minutes. Thawed samples were sonicated for six-ten second intervals at 95% power (Sonicator Ultrasonic Processor XL, Heat Systems), passed twice through both 21 and 25 gauge needles (Becton-Dickson), and centrifuged at 21,000 rpm at 4^{o}C (Eppendorf Centrifuge 5810R).

PURIFICATION OF HISMIPS FUSION PROTEINS

Recombinant HISMIPS protein was purified using metal affinity chromatography. This procedure consists of (1) binding of the lysate, (2) washing of the beads, and (3) eluting of the product. First, a slurry of 50% (v/v) nickel-nitrilotriacetic acid metal affinity chromatography matrix (Ni^{2+}-NTA agarose bead) (Qiagen) was equilibrated in an equal column volume of denaturing lysis buffer. The cell lysate was bound to the Ni^{2+}-NTA agarose beads by adding 1 ml of beads per 4 ml of HISMIPS lysate according to the manufacturer's instructions (Qiagen) and agitating at RT for 30 minutes. The bead/lysate

mixture was centrifuged (Eppendorf Centrifuge 5810R) for 30 seconds at 700 relative centrifugal force (rcf) and the supernatant was decanted. The beads were washed twice with an equal volume of denaturing wash buffer (8 M urea, 0.1 M sodium phosphate and 0.01 M Tris-HCl pH 6.3). The HISMIPS protein was eluted using four column volumes of denaturing elution buffer (8 M urea, 20 mM imidazole, 0.1 M sodium phosphate buffer, and 0.01 M Tris-HCl pH 4.5). Elution products were stored at –20^{o}C.

DIALYSIS OF HISMIPS PROTEIN

The HISMIPS elution product was dialyzed against Phosphate Buffered Saline (PBS: 1.5 M NaCl, 26.8 mM KCl, 100 mM Na_2HPO_4, 17.6 mM KH_2PO_4) with decreasing concentrations of urea. The product was dialyzed for 2 hours at RT in a colloidal membrane (Schleicher and Schuell) with 6, 4, and 2 M urea. The elution product formed a precipitate and the solution became cloudy and particulate. The solution and precipitate were removed, and the membrane was rinsed with 2 ml of PBS. The HISMIPS protein product was lyophilized (courtesy of Dr. Thomas Sitz, Virginia Polytechnic Institute and State University) and stored at -20^{o}C.

ANTIBODY PRODUCTION

The lyophilized protein was shipped to a commercial antibody production facility (CoCalico Biologicals, Inc., Reamstown, PA). One female rabbit was chosen to produce the rabbit-anti-*Gm*MIPS antiserum. The rabbit received antigen inoculations and bleeds as prescribed by a standard protocol (CoCalico Biologicals Inc.). Each inoculation consisted of 175 μg of antigen. The pre-bleed and initial inoculation using RIBI adjuvant (RIBI Immunochem Research, Inc.) was completed on day zero. The first and second boosts were completed at day 14 and 21. A test bleed (test bleed #1) was taken at day 35. A fourth boost was given on day 49; test bleed #2 was collected on day 56. A final inoculation was delivered on day 73, and a terminal bleed was performed on day 87. The rabbit anti-*Gm*MIPS antiserum was stored at –80^{o}C.

SDS-PAGE

Proteins were visualized using SDS-PAGE as described by Laemmli (1970). Electrophoresis was performed using a mini-protean II unit (Bio-Rad). Samples of 1-20 µg (20-30 µl) were prepared by diluting the proteins in SDS-PAGE sample buffer (30% (v/v) glycerol, 190 mM Tris-HCl pH 6.8, 5 mM EDTA, 7% (w/v) SDS, 0.1% Bromophenol Blue, 15% (v/v) 2-mercaptoethanol). Samples were electrophoresed at 175 volts for approximately 1 hour in SDS-PAGE running buffer (125 mM Tris-HCl, 959 mM glycine, 0.1% (v/v) SDS). The gels were stained with Coomassie Brilliant Blue (50% methanol, 0.04% (v/v) Coomassie Brilliant Blue R-250, 10% (v/v) acetic acid).

ELECTROTRANSFER OF PROTEINS

Proteins were transferred to nitrocellulose using either the semi-dry technique or the wet tank technique. The semi-dry technique employed a trans-blot semi-dry electrophoretic transfer cell (Bio-Rad), and the wet tank technique used the mini-trans-blot electrophoretic transfer cell (Bio-Rad). For semi-dry transfer, the SDS-polyacrylamide gel was rinsed in semi-dry transfer solution (48 mM Tris-HCl, 39 mM glycine, 0.0375% SDS and 20% methanol) for two minutes. The polyacrylamide gel was applied to a stack of 3 mm Whatman chromatography paper (Fisherbrand), and one sheet of 0.45 µm pure nitrocellulose (Trans-Blot Transfer Medium, Bio-Rad) and covered with five sheets of 3 mm Whatman chromatography paper. Each component of the transfer stack was pre-wetted in semi-dry transfer buffer. The proteins were transferred to the filter at 15 volts for 30 minutes.

Gels for transfer using the wet tank technique were rinsed in wet tank transfer buffer (25 mM Tris-HCl, 192 mM glycine and 20% (v/v) methanol). A transfer sandwich was made and inserted into a transfer cassette. The transfer sandwich consisted of a fiber pad, one piece of 3 mm Whatman chromatography paper (Fisherbrand), the gel, 0.45 µm pure nitrocellulose, 3 mm Whatman chromatography paper and a final fiber pad; each

component was saturated in wet tank transfer buffer. The cassettes were added to the tank and electrophoresed overnight at 4°C at a constant voltage of 30 Volts.

DETECTION USING Ni^{2+}-ALKALINE PHOSPHATASE CONJUGATE

The Ni^{2+}-Alkaline Phosphatase-conjugate (Ni^{2+}-AP-conjugate) (Qiagen) was used for HISMIPS detection. The filter was blocked in 5% blotting grade blocker non-fat dry milk (Bio-Rad) and Tris Buffered Saline with Tween (TBST: 20 mM Tris, 150 mM NaCl, 0.05% (v/v) Tween 20) for 20 minutes at RT. The Ni^{2+}-AP-conjugate was diluted 1:1000 in TBST and incubated at 4°C overnight. The filter was washed in TBST three times for seven minutes each at RT and equilibrated in Alkaline Phosphatase Buffer (APB; 100 mM Tris, 100 mM NaCl, 5 mM $MgCl_2$, pH 9.5). Equilibrated filters were treated with a SIGMA-FAST NBT/BCIP substrate (0.15 mg/ml 5-bromo-4-chloro-3-indolyl phosphate, 0.3 mg/ml nitro blue tetrazolium, 100 mM Tris-HCl, 5 mM $MgCl_2$) and rocked in the solution at RT in the dark until a purple precipitate appeared on the filter.

PROTEIN BLOTTING

Protein transfer was detected using the reversible protein stain, Ponceau S (5 mg/ml Ponceau S, 1% glacial acetic acid (v/v)). The filter was washed in two changes of deionized/distilled water for ten minutes followed by one wash in PBST (PBS and 0.1% Tween-20) for twenty minutes. After completely removing the Ponceau S, the filter was blocked for three hours at RT in blocking solution (5% blotting grade blocker non-fat dry milk and PBST). The primary antibody, rabbit-anti-*Gm*MIPS-antiserum (anti-*Gm*MIPS-antiserum) was diluted in fresh blocking solution and incubated for one hour at RT with agitation in a small plastic bag. The filter was washed in 100 ml of PBST per filter, once briefly in PBST and then three times for fifteen minutes each at RT. The primary antiserum was stored at 4°C with 0.01% sodium azide for further use. The secondary antibody, goat anti-rabbit IgG conjugated to horseradish peroxidase (Bio-Rad), was applied to the filter at a dilution of 1:3000 and incubated for forty-five minutes at RT

followed by three washes as above. Signal detection was carried out using an ECL^{+}Plus Kit (Amersham Pharmacia Biotech) as directed by the manufacturer.

GEL ASSAY QUANTIFICATION

Protein was visually quantified by direct comparison to BSA standards. Various amounts of BSA (50 ng, 100 ng, 150 ng, 200 ng, 250 ng and 1000 ng) and elution product (1 µl, 5 µl and 10 µl) were separated by SDS-PAGE and stained with Coomassie Brilliant Blue. Elution product aliquots were visually compared to the BSA standards to estimate protein quantity.

PLANT PROTEIN EXTRACTIONS

100 mg of plant tissue was ground to a fine powder in approximately 25 ml of liquid nitrogen and transferred to a 1.5-ml Eppendorf tube. The powder was resuspended in 1 ml of homogenizing buffer (0.15 M KCl, 0.050 M Tris-HCl, pH 8.0, and 0.0005 M EDTA) and vortexed. Protease and phosphatase inhibitor cocktail for plant cell extracts (Sigma) was added to a concentration of 3.3 µl/mg of plant tissue. Protease and phosphatase inhibitor cocktail for plant cell extracts contains 4-(2-aminoethyl) benzenesulfonyl fluoride (AEBSF), bestatin, pepstatin A, trans-epoxysuccinyl-L-leuclamido (4-guanidino) butane (E-64), leupeptin and 1,10-phenanthroline. The extract was homogenized using an ice-cold dounce homogenizer. Triton X-100 was added to a final concentration of 0.1% before samples were centrifuged at 14,000 x g for 10 minutes at 4^{o}C. The clear supernatant was removed, aliquoted and frozen at –80^{o}C.

NITROCELLULOSE STRIP PURIFICATION OF THE ANTI-GmMIPS ANTISERUM

The crude anti-*Gm*MIPS antiserum was rapidly purified using a nitrocellulose strip method. A preparatory 10% SDS-polyacrylamide gel was used to separate total protein extracts made from IPTG-induced bacteria containing the pEThisMIPS construct. The gel was transferred to nitrocellulose (see above) using a semi-dry transfer apparatus. The HISMIPS protein was visualized using the reversible Ponceau S stain, and the 76 kD

band was cut from the filter, producing a 5 cm strip of nitrocellulose. The strip was incubated with crude anti-*Gm*MIPS antiserum at a dilution of 1:100,000 in TBST and 5% blocking solution for 1 hour. The primary antiserum was removed and the strip was washed in TBST 3 times for 7 minutes each at RT. The antibodies bound to the filter strip were eluted using 4 M $MgCl_2$. The elution product was dialyzed against PBS for two 3-hour changes at 4°C and stored in 40% glycerol and 1% Bovine Serum Albumin (BSA).

PREPARATION OF ANTI-GmMIPS ANTISERUM FOR AFFINITY PURIFICATION

Crude antiserum from the terminal bleed was centrifuged at 3000 rcf at 4°C for 30 minutes. The supernatant was removed and added to a small Erlenmeyer flask with a magnetic stir bar. 4.1 M ammonium sulfate was added drop-wise to the antibody solution to a final concentration of 50% (v/v). The flocculent solution was transferred to a new tube and incubated at 4°C for six hours. The subsequent antiserum was centrifuged at 3000 rcf for thirty minutes. Anti-*Gm*MIPS antiserum was resuspended in PBS, 40% glycerol and 1% Bovine Serum Albumin (BSA).

AFFINITY PURIFICATION OF THE ANTI-GmMIPS ANTISERUM

The anti-*Gm*MIPS antiserum was purified using a subtractive column. A plasmid that expressed a histidine tagged mutant POLYHIS*NIFU* protein (kindly provided by D. Dean, Virginia Polytechnic Institute and State University) was transformed into *E. coli* strain BL 21 (DE 3). A 5 ml overnight culture of the transformed cells was diluted in 100 ml of LB broth with 50 μg/ml ampicillin. The cells were grown to a Klett = 160 (Klett-Summerson Photoelectric Colorimeter) and induced with 0.4 mM IPTG for two hours. The cells were centrifuged at 4000 rpm for 20 minutes. The cell pellet was resuspended in borate buffer pH 9.0 (67 mM borax, 33 mM boric acid, pH 9.0-9.5) with 1 mg/ml lysozyme (Sigma) and incubated on ice for 15 minutes. Dn*ase*I (Sigma) was added to a final concentration of 5 μg/ml and rocked gently for 1 hour at 4°C. The lysate was passed twice through both 21 and 25 gauge needles.

Next, the concentration of the total protein extract was determined using a Bradford Assay Kit (Bio-Rad). Using the manufacturer's instructions, a standard curve was made using concentrations of lyophilized bovine plasma gamma globulin (Bio-Rad protein assay standard). A Beckman Spectrophotometer was used to determine the absorbance at 595 nm. Sample absorbances were plotted on the standard curve to determine total protein concentrations in mg/ml.

Total protein extract prepared from bacteria containing the pPOLYHIS*NIFU* construct was bound to 1, 1' –Carbonyldiimidazole activated beads (Reacti-gel, Pierce) and used to prepare a purification column. The Reacti-gel (Pierce) was added to 10 ml of ice-cold water, gently rocked for 30 seconds, and centrifuged for 10 seconds at 4000 rpm. The supernatant was removed and the beads were washed twice in 10 ml of ice-cold sterile water. Total protein extract (20 mg) was diluted to a final volume of 5 ml in borate buffer and added to the Reacti-gel beads (Pierce) at a final concentration of 1 ml of beads per 5 ml of protein extract. The bead/extraction solution was rocked overnight at RT, according to the manufacturer instructions. After the protein solution was removed, the matrix binding sites were quenched with 2 M Tris-HCl pH 8.0. The beads were packed into a column, washed with several changes of PBS and stored overnight at 4^{o}C.

The subtractive column was prepared for application of antiserum. First, the packed column was washed with 10 ml of PBS and 10 ml of 6 M guanidine hydrochloride in PBS. The column was mock eluted with 4 M $MgCl_2$ and washed with 20 ml of PBS. The crude diluted antiserum was passed over the column multiple times at RT. After the affinity purified anti-*Gm*MIPS antiserum was collected, the column was washed at RT with PBS, 1 M guanidine hydrochloride in PBS and 4 M $MgCl_2$. The used subtractive column was stored in PBS and 0.01% sodium azide at 4^{o}C.

STORAGE OF ANTI-GmMIPS ANTIBODY

The pre-bleed and each test bleed were received frozen in dry ice from CoCalico Biological Inc. Crude antiserum was stored at 4^{o}C until first tested, then it was transferred to 1-ml aliquots and permanently stored at –80^{o}C.

RESULTS

MIPS PRIMARY PROTEIN STRUCTURES ARE CONSERVED

Predicted amino acid sequences of *At*MIPS-1 (Johnson, 1994) and -2 (Johnson and Burk, 1995), *Bn*MIPS (Hussain et al., 1997), *Gm*MIPS (Hegeman, unpublished data), *Hv*MIPS (Larson and Raboy, 1998) *Mc*MIPS (Ishitani, et al., 1996), *Np*MIPS (Hashimoto et al., 1999), *Os*MIPS (Yoshida et al., 1999), *Sp*MIPS (Smart and Fleming, 1993), *Sc*MIPS (Johnson et al., 1989), *Ta*MIPS (Hussain, 1999) and *Zm*MIPS (Larson and Raboy, 1998) (Table 1.1) were analyzed and assembled in a phylogenetic tree using the CLUSTAL method (Thomspon et al., 1994) in the computer program MegAlign (Lasergene Software, DNAstar) (Figure 2.1). The phylogenetic tree indicates the relationship between the MIPS amino acid sequences from each species relative to one another; each step of the analysis marks a dichotomous branching that produces two genetically separated sister branches that are equal to each other in rank, or percentage divergence. The proteins found on the same branch make up the sister taxa, or related proteins. Analysis of MIPS proteins indicates that the plant MIPS are closely related and do not exceed 8% divergence. The yeast MIPS, *Sc*MIPS is closely related to the plant MIPS (38.5% divergence). However, *Sc*MIPS occupies a phylogenetic branch separate from the plant MIPS proteins, which occupy a single branch. The separation of the plant MIPS amino acid sequences corresponds to three branches: a dicot branch (*At*MIPS-1 (Johnson, 1994) and -2 (Johnson and Burk, 1995), *Bn*MIPS (Hussain et al., 1997), *Ta*MIPS (Hussain, 1999), *Mc*MIPS (Ishitani et al., 1996) *Gm*MIPS (Hegeman et al., unpublished data) and *Np*MIPS (Hashimoto et al., 1999)), a monocot branch (*Hv*MIPS (Larson and Raboy, 1998), *Os*MIPS (Yoshida et al., 1999) and *Zm*MIPS (Larson and Raboy, 1998)) and an aquatic plant MIPS protein, *Sp*MIPS (Smart and Fleming, 1993).

The specific aim of this research was to develop a tool to study MIPS protein expression in plants. Due to the high sequence similarity between the predicted amino acid sequences of *mips* genes, we considered it likely that antiserum raised against one plant MIPS protein would cross-react with MIPS proteins from other plants (Figure 2.1). *At*MIPS-1 (Johnson, 1994), *At*MIPS-2 (Johnson and Burk, 1997) and *Gm*MIPS

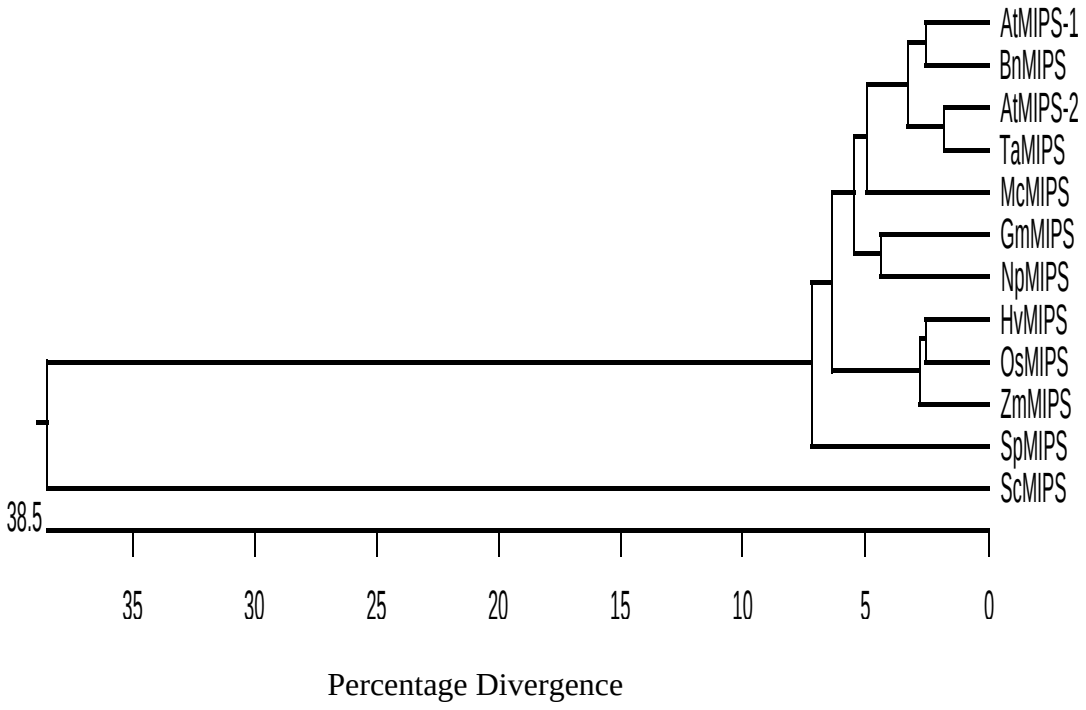

Figure 2.1 Phylogenetic analysis of predicted amino acid sequences from plants and yeast (*Saccharomyces cervisiae*). The predicted amino acid sequences for MIPS genes from *Arabidopsis thaliana* (*At*MIPS –1) (Johnson, 1994) (*At*MIPS-2) (Johnson and Burk, 1995), *Brassica napus* (*Bn*MIPS) (Hussain et al.,1997), *Glycine max* (*Gm*MIPS) (Hegeman et al., unpublished data), *Hordeum vulgare* (*Hv*MIPS) (Larson and Raboy, 1998), *Mesmbryanthemum crystallinum* (*Mc*MIPS) (Ishitani et al., 1996), *Nicotiana paniculta* (*Np*MIPS) (Hashimoto et al., 1999), *Oryza sativa* (*Os*MIPS) (Yoshida et al., 1999), *Spirodela polyrrhiza* (*Sp*MIPS) (Smart and Fleming, 1993), *Triticum aestivum* (*Ta*MIPS) (Hussain, 1999), *Sacchromyces cervisi*ae (*Sc*MIPS) (Johnson and Henry, 1989) and *Zea mays* (*Zm*MIPS) (Larson and Raboy, 1998) were aligned using the CLUSTAL method (Thompson et al., 1994) in the computer program MegAlign (Lasergene Software, DNAstar). The scale at the bottom is percentage divergence. Lower numbers show a closer relationship between organisms. Predicted molecular masses can be found in Table 1.1.

(Hegeman et al., unpublished data) predicted amino acid sequences were compared using the CLUSTAL method (Thompson et al., 1994) in the computer program MegAlign (Lasergene Software, DNAstar). The alignment of these predicted amino acid sequences indicates the three sequences are nearly identical (86.7% between *At*MIPS-1 and *Gm*MIPS and 86.9% between *At*MIPS-2 and *Gm*MIPS) (Figure 2.2). Note that (1) many amino acids that are not identical are conserved and (2) that there are no more than three amino acid residues in a row that are not identical.

Due to both the low percentage divergence between MIPS sequences of many different species and the close identity of the predicted amino acid sequences of Arabidopsis and soybean, it was highly probable an antiserum raised against *Gm*MIPS would cross react with the *At*MIPS isoforms. Previously, a portion of the cDNA sequence of *Gmmips* was fused to a 6X-histidine tag in the overexpression vector, pET32a (+). The resulting plasmid was transformed into cell line pLYSs and provided by C. Hegeman and E. Grabau (Virginia Polytechnic Institute and State University). The transformed cells were induced with IPTG in order to overexpress the recombinant protein, HISMIPS, to be later used as an antigen for the production of anti-*Gm*MIPS antiserum.

OVEREXPRESSION OF RECOMBINANT HISMIPS IN A BACTERIAL SYSTEM

Recombinant protein overexpression parameters were optimized to for a yield of high purity antigen. Separate cell cultures were incubated at two optical densities (OD_{600} = 0.1 and 0.6) prior to IPTG induction. Induction at an OD_{600} = 0.1 proved to yield more HISMIPS as determined visually using the Ni^{2+}AP-conjugate (Qiagen) (data not shown). The yield of HISMIPS protein was also related to the length of incubation and growth temperature. Cells were incubated at RT and 37^{o}C for 3 and 10 hours. Incubation of cells at RT for 10 hours allowed for nearly 2X more extractable HISMIPS than the other three conditions. Therefore, increasing culture incubation times and decreasing the temperature at which cells were cultured post IPTG induction greatly increased the yield of HISMIPS (Figure 2.3A).

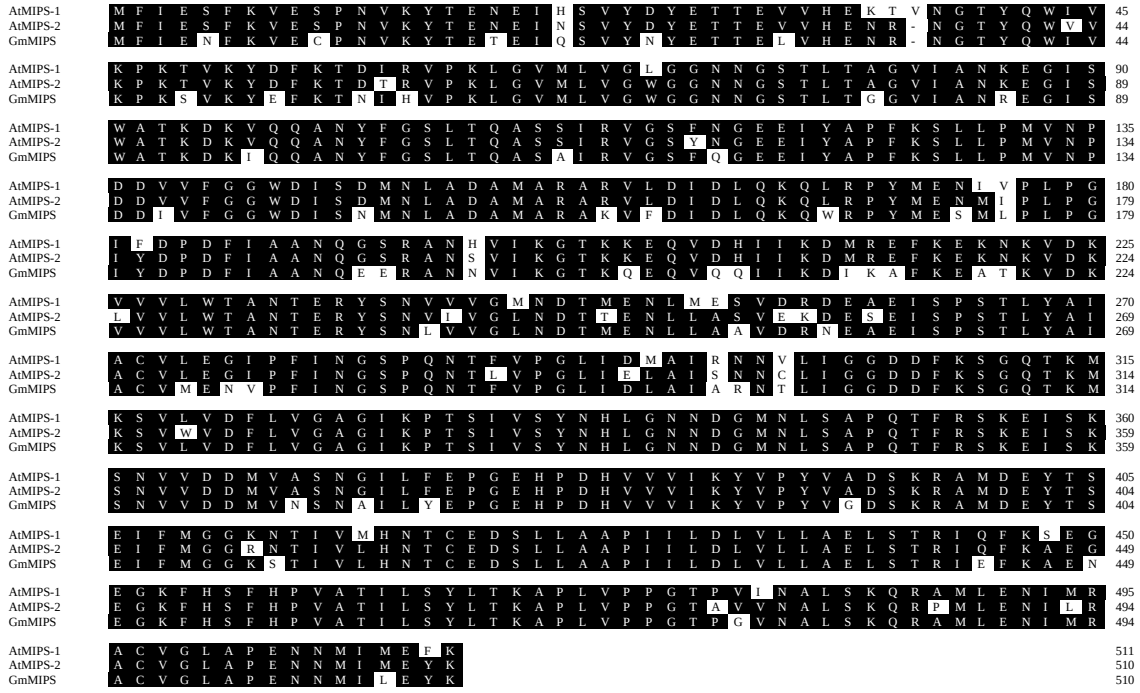

Figure 2.2 Predicted amino acid sequences of *At*MIPS-1, -2 and *Gm*MIPS.

Sequences were aligned using the CLUSTAL method (Thompson, 1994) in the computer program MegAlign (Lasergene Software, DNAstar). Shaded boxes indicate conserved amino acids . *At*MIPS-1 and -2 show significant amino acid conservation with *Gm*MIPS.

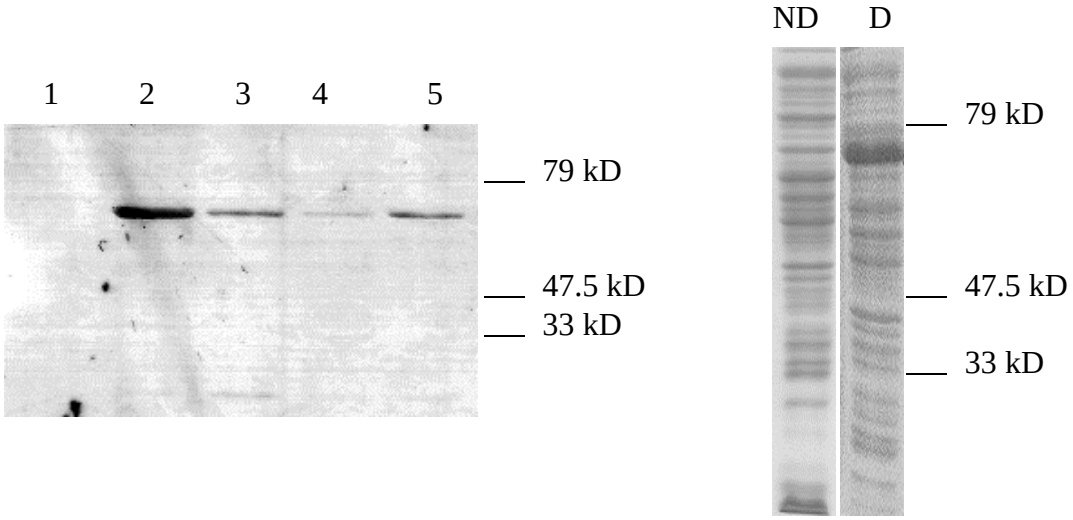

Figure 2.3 Optimization of time, temperature and solubility for the overexpression and extraction of HISMIPS. (A) Untransformed control bacteria (1) and bacteria containing the construct pEThisMIPS were grown at RT for 10 hours (hrs) (2), RT for 3 hrs (3), 37^{o}C for 3 hrs (4) and 37^{o}C for 10 hrs (5) at OD_{600} = 0.1. Migration of pre-stained molecular weight markers are shown on the right. Total protein extracts were made using a non-denaturing lysis buffer, separated by SDS-PAGE, transferred to nitrocellulose and detected using a Ni^{2+}-AP-conjugation. The Ni^{2+}-AP-conjugate detects the 76 kD fusion protein in bacterial extracts. Lanes are equally loaded as quantified on a gel stained with Coomassie Brilliant Blue. These results indicate cells grown OD_{600} = 0.1 express the most protein during a 10 hour incubation at room temperature. These optimized conditions were used in further experiments to express the protein. (B) Bacteria containing the HISMIPS construct were grown at conditions determined in (A) and extracts were made using either non-denaturing (ND) or denaturing (D) lysis buffer. Proteins were separated on SDS-PAGE and visualized with Coomassie Brilliant Blue Stain.

Additionally, denaturing conditions for protein extraction greatly increased the amount of extractable HISMIPS protein. Denaturing conditions made the cell proteins soluble and produced over 10X more extractable HISMIPS protein than soluble extraction procedures (Figure 2.3B).

The recombinant protein, HISMIPS, was overexpressed in a prokaryotic expression system. The predicted size of HISMIPS was 70 kD, however, the fusion protein migrated slower than 70 kD. The apparent molecular mass of HISMIPS, 76 kD, was calculated from a standard curve using pre-stained molecular mass markers. Size discrepancy between the predicted and apparent molecular masses may be due to the bulkiness of the 6X-histidine tag.

AFFINITY PURIFICATION OF HISMIPS

Metal affinity chromatography was performed to obtain recombinant protein of the highest purity possible. Total HISMIPS protein lysate was incubated with Ni^{2+}-NTA agarose beads such that the histidine tag would bind to the multivalent nickel. After the recombinant protein was bound, the column was washed, and HISMIPS was eluted. Purification procedures were optimized for the highest yield and purity by adding 20 mM imidazole to the wash buffer and decreasing the bead/protein binding time to 30 minutes (data not shown). The 76 kD recombinant protein was observed in each purification step starting with the total protein extract (Figure 2.4). The unbound lane indicates those proteins that did not bind to the Ni^{2+}-NTA agarose beads. The column was washed in denaturing buffer pH 6.3, which cleared the beads of non-specific binding. This protein was of high purity. Approximately 700 μg of HISMIPS protein was purified, lyophilized and shipped to a commercial antibody production facility. After elution, 1% of the Ni^{2+}-NTA agarose beads were resuspended in Laemmli buffer. Gel assay quantification (see materials and methods) indicated approximately 1 mg of protein could be further eluted.

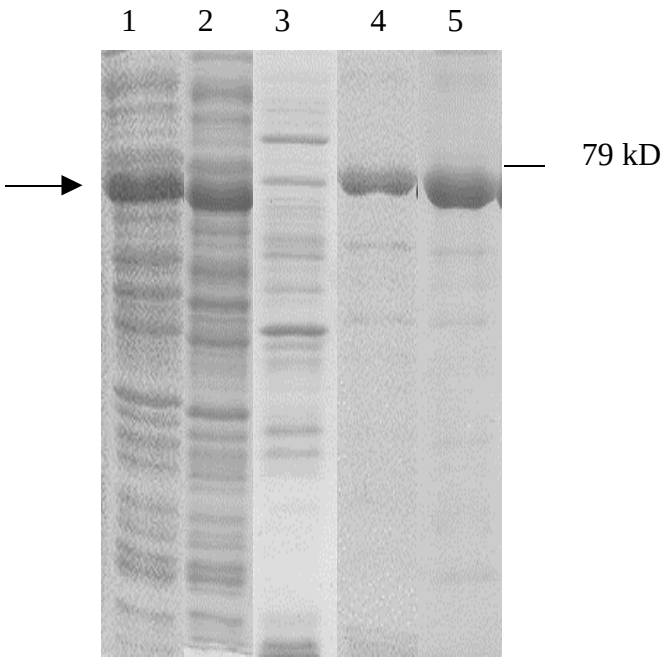

Figure 2.4 HISMIPS overexpression and purification. The recombinant protein HISMIPS was purified using metal affinity chromatography. Aliquots from each purification step were resuspended in Laemmli buffer, separated by SDS-PAGE and stained with Coomassie Brilliant Blue. Each lane is representative of an individual purification procedure. Lanes are denoted as follows: Total Extract (1), Unbound (2), Wash (3), Elution Product (4), Beads (5). The black arrow indicates the 76 kD HISMIPS fusion protein. Approximately 700 μg of HISMIPS was eluted.

CRUDE ANTI-GmMIPS ANTISERUM CHARACTERIZATION

The HISMIPS recombinant protein was used as an antigen to produce anti-*Gm*MIPS antiserum. One female rabbit was inoculated with 175 μg of antigen at a commercial antibody production facility (CoCalico Biologicals). Two test bleeds and one terminal bleed were taken from the animal after five injections of antigen with RIBI-immune advajunt. The serum was separated from the whole blood.

Characterization of the anti-*Gm*MIPS antiserum involves determining antiserum cross-reactivity with the antigen and proteins from the plant species, Arabidopsis and soybean. First, crude antiserum was used in protein blot analysis using total bacterial protein extracts from both the HISMIPS bacterial line and bacteria containing the pBluescriptSK (+) (plasmid control) (Figure 2.5A). A series of anti-*Gm*MIPS antiserum dilutions were tested. Antiserum was diluted in either TBST or PBST (see materials and methods) with 5% (w/v) dry non-fat milk (Bio-Rad) at ratios of 1:500, 1:1000, 1:1500, 1:2000, 1:5000, 1:25,000, 1:50,000 (data not shown) and 1:100,000. The blots performed at higher antiserum dilution ratios showed high background, however, the 1:100,000 dilution allowed for the detection of one band at 76 kD with very low background in the HISMIPS lane and no bands in the plasmid control lane (Figure 2.5A). Next, the anti-*Gm*MIPS antiserum was tested against Arabidopsis and soybean total protein extracts. Crude total protein extracts were separated by SDS-PAGE, transferred to nitrocellulose using a semi-dry transfer technique and blotted using anti-*Gm*MIPS antiserum diluted to 1:100,000. Figure 2.5B indicates the antiserum detected a soybean protein with an apparent molecular weight of 64 kD. *At*MIPS was not detectable using the crude antiserum. However, a smaller Arabidopsis protein with an apparent molecular weight of 34 kD was found. Therefore, it was necessary to purify the antiserum.

ANTI-GmMIPS ANTISERUM NITROCELLULOSE STRIP PURIFICATION

In an effort to rapidly purify the anti-*Gm*MIPS antiserum, crude antiserum was bound to a nitrocellulose strip containing bacterial extracts prepared from pLYSs cells

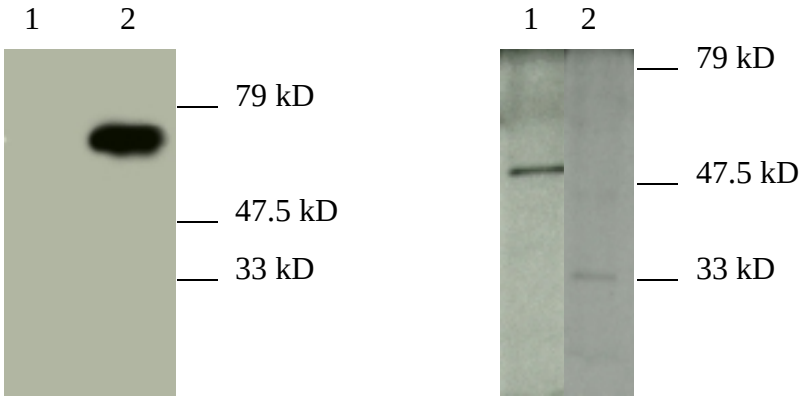

Figure 2.5 Protein blot of recombinant HISMIPS, soybean and Arabidopsis total protein extracts using crude antiserum. Total protein extracts were separated on SDS-PAGE and transferred to nitrocellulose using a semi-dry transfer apparatus. Crude antiserum was diluted to 1:100,000 in TBST and 5% blotting grade blocker non-fat dry milk (Bio-Rad). (A) Crude anti-*Gm*MIPS antiserum detects the 76 kD recombinant HISMIPS protein (2) and does not detect a signal in the plasmid control lane (1). (B) A *Gm*MIPS protein at 64 kD was detected in young soybean protein (1) extracts using crude antiserum, however, the Arabidopsis ortholog was not detected (2). Approximately 25 µg of plant protein was loaded in each lane.

containing the pEThisMIPS construct. Following incubation, the filter was washed to remove impurities and the anti-*Gm*MIPS antiserum was eluted. A preparative polyacrylamide gel with approximately 100 mg of HISMIPS total extract was transferred to nitrocellulose (see materials and methods). The band of interest was cut from the filter and incubated with crude antiserum at a dilution of 1:100,000. The anti-*Gm*MIPS antiserum was eluted from the strips using $MgCl_2$. The cross reactivity of the nitrocellulose strip purified antibody was tested against the plasmid control, HISMIPS crude total bacterial protein extracts, dark grown Arabidopsis, light grown Arabidopsis, and immature soybean seed proteins (Figure 2.6A). Although the antiserum cross-reacted with the recombinant protein, no background bands were detected in the plasmid control. Unfortunately, detection of *At*MIPS and *Gm*MIPS was not enhanced in plant extracts as expected. Interestingly, the nitrocellulose strip purification did enhance the detection of the 34 kD band, previously found in light grown Arabidopsis seedlings.

Although the identity of the 34 kD protein is not clear, it may be an artifact of using a histidine tagged protein for antiserum production. A BLAST search of the Arabidopsis genome project using nine tandem histidine residues results in greater than 50 peptides with this repeat. These proteins range in function from heat shock proteins to a putative pectin methylesterase.

In order to determine if this protein could be a metal binding protein, Arabidopsis light grown seedling total protein extracts were incubated with Ni^{2+}-NTA agarose beads. An aliquot of the beads, approximately 1%, were resuspended in Laemmli loading buffer and separated by SDS-PAGE. Duplicate nitrocellulose filters were produced in order to analyze the flow through (unbound) and bound bead (bound) products using both Ni^{2+}-AP-conjugate (data not shown) and the filter strip purified anti-*Gm*MIPS antiserum. Both the Ni^{2+}-AP-conjugate (data not shown) and the antiserum detected a 34 kD protein in the bead lane (Figure 2.6B). Nevertheless, the nitrocellulose strip purified antiserum could not be used to detect the *At*MIPS protein, and further protein blot optimization and antiserum purification techniques, such as affinity purification by subtractive column, were necessary.

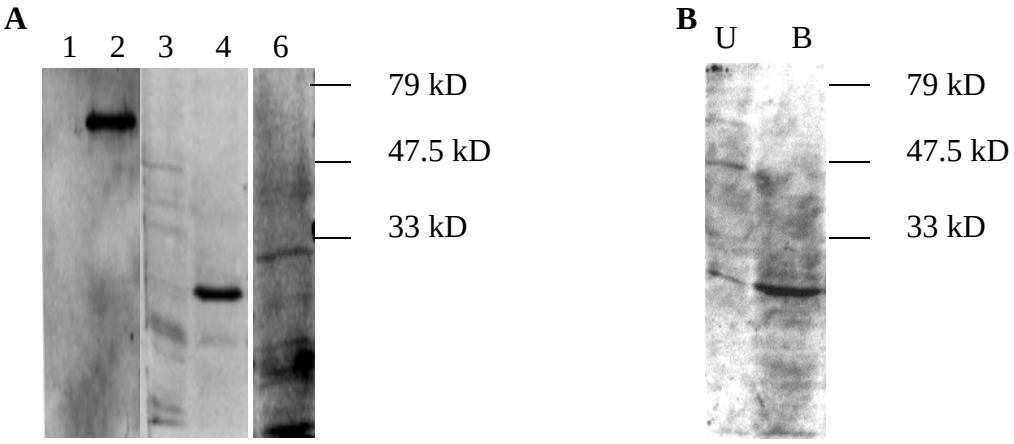

Figure 2.6. Protein blots using strip purified anti-*Gm*MIPS antiserum. Bacterial and plant crude protein extracts were separated by SDS-PAGE and transferred to nitrocellulose using a semi-dry transfer method. Filters were incubated with anti-MIPS antiserum at 1:500 dilution in TBST and 5% milk. (A) Composite western blots using the strip purified anti-*Gm*MIPS antiserum. (1) SK (bacterial negative control), (2) HISMIPS total protein extract, (3) dark grown (DG) Arabidopsis seedlings, (4) light grown (LG) Arabidopsis seedlings and (5) immature soybean seeds were analyzed. The black arrow denotes the 76 kD recombinant HISMIPS protein and the gray arrow indicates the 34 kD detected plant protein. (B) To test whether the strip purified antiserum detects histidine containing proteins, plant total protein extracts were incubated with Ni^{2+}-NTA agarose beads, and bound (B) and unbound (U) proteins were separated by SDS-PAGE. After transfer to nitrocellulose, and blotted using the strip purified anti-*Gm*MIPS antiserum at a dilution of 1:500. The gray arrow denotes the 34 kD histidine-containing protein that is detected in the bound lane and not the unbound lane.

PROTEIN TRANSFER OPTIMIZATION FOR DETECTION OF AtMIPS

Protein transfer to nitrocellulose can be accomplished using either a semi-dry system or a wet tank system. Although semi-dry transfer is often preferred due to short transfer times, larger proteins may be better transferred by the wet system. In a parallel study conducted by L. Good and E. Grabau (Virginia Polytechnic Institute and State University) using the anti-*Gm*MIPS antiserum, *Gm*MIPS protein was readily detectable in immature soybean proteins using the wet tank transfer technique. Therefore, total protein extracts from young soybean seeds (positive control) and light and dark grown Arabidopsis seedlings (approximately 25 μg of crude extract) were transferred using the wet tank technique. This transfer technique was successful for the detection of both *At*MIPS and *Gm*MIPS (Figure 2.7). The *At*MIPS protein was also detectable in dark grown Arabidopsis seedlings, however it accumulated at a much lower level than the *At*MIPS detected from light grown seedlings. Although this transfer technique, coupled with lower anti-*Gm*MIPS antiserum dilution, indicates *At*MIPS is detectable using the crude antiserum, the increase in background bands further necessitated affinity purification of the antiserum.

AFFINITY PURIFICATION OF ANTI-GmMIPS ANTISERUM

In order to remove background, anti-*Gm*MIPS antiserum was purified by subtractive chromatography. Proteins from BL21 cells containing the pPOLYHIS*NIFU* construct were covalently bound to a 1, 1' –Carbonyldiimidazole activated bead matrix and packed into a column. When the crude antiserum was passed over the beads, non-anti-*Gm*MIPS antibodies cross-react with the protein/bead matrix and become trapped within the column. The anti-*Gm*MIPS antibodies will not cross react with the protein/bead matrix and pass through the column. This procedure produced affinity purified anti-*Gm*MIPS antiserum (Figure 2.8A).

The affinity purified anti-*Gm*MIPS antiserum was used to detect *At*MIPS and *Gm*MIPS from crude total protein extracts. Protein blots were probed with the purified

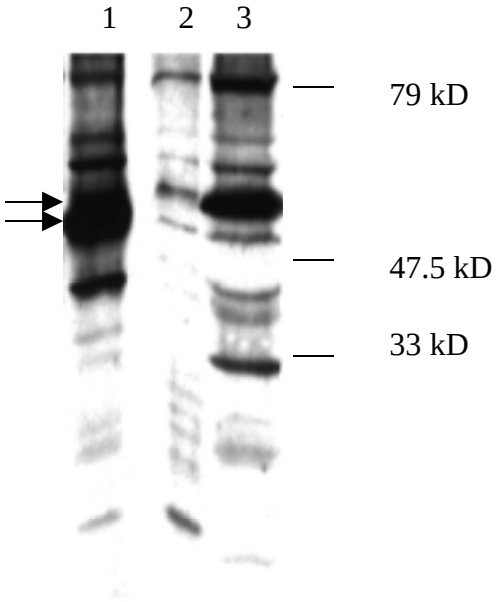

Figure 2.7 Protein blot of total protein extracts using a tank transfer. Total protein extracts were transferred overnight using a wet tank transfer apparatus. Protein from immature soybean seed (1), dark grown (DG) Arabidopsis seedlings (2) and light grown (LG) Arabidopsis seedlings (3) were analyzed using the crude antiserum at a dilution of 1:10,000. The upper black arrow denotes *At*MIPS and the lower arrow denotes *Gm*MIPS. Lanes contain approximately 30 μg of crude protein extract. Using this method for transferring proteins, the crude anti-*Gm*MIPS antiserum readily detects the *At*MIPS.

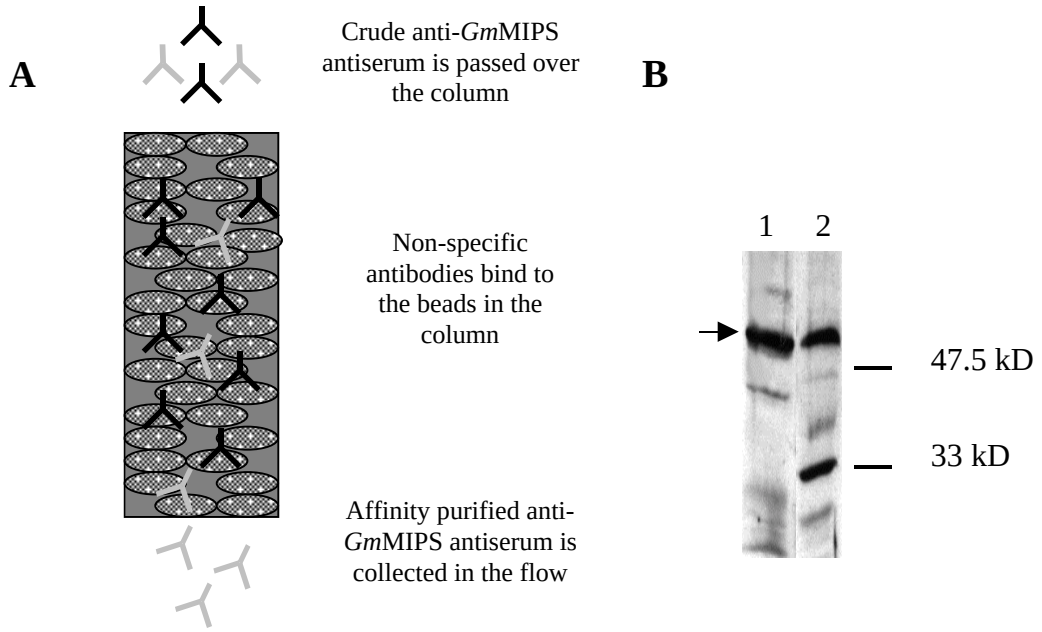

Figure 2.8 Procedure and protein blot using affinity purified anti-*Gm*MIPS antiserum. (A) To remove non-specific antibodies, total protein extract was isolated from *E. coli* containing a pPOLYHIS*NIFU* construct and bound to a solid matrix (Reacti-gel). The crude anti-*Gm*MIPS antiserum was passed over the column. Non-*Gm*MIPS antiserum was trapped in the column and the anti-*Gm*MIPS antibodies were collected in the flow through and used in B. (B) Total protein extracts from immature soybean seeds and light grown (LG) Arabidopsis seedlings were separated by SDS-PAGE, wet tank transferred to nitrocellulose and blotted using a 1:37,500 dilution of affinity purified anti-*Gm*MIPS antiserum. The black arrow notes both *Gm*MIPS (apparent molecular mass 64 kD) and *At*MIPS (apparent molecular mass 66 kD). This purification has reduced background signals previously obtained with the crude antiserum.

antiserum at dilutions of 1:250, 1:500, 1:1000, 1:15,000, 1:20,000 (data not shown) and 1:37,500. Purifying the antiserum resulted in less background. Additionally, *At*MIPS was more readily detectable and one or more isoforms with apparent molecular weights of 65-66 kD may be present (Figure 2.8B).

DEVELOPMENTAL ANALYSIS OF AtMIPS PROTEINS

The affinity purified anti-*Gm*MIPS antiserum was used in a protein blot analysis of different Arabidopsis tissues and developmental stages to determine *At*MIPS protein accumulation (Figure 2.9). MIPS protein was previously found to be developmentally regulated in green bean (Johnson and Wang, 1996) and soybean (Hegeman et al., unpublished). One *At*MIPS protein was detected in crude total protein extracts after separation by SDS-PAGE. The protein accumulation pattern confirms *At*MIPS is developmentally regulated. *At*MIPS was found at the highest levels in opened flowers, unopened flowers, and one-month-old light grown Arabidopsis seedlings. Siliques, and two-week-old light grown Arabidopsis seedlings accumulate low levels of *At*MIPS. Interestingly, the 34 kD protein is also developmentally regulated.

AtMIPS PROTEINS DIFFERENTIALLY ACCUMULATE IN SILIQUES

The HISMIPS recombinant protein was the product of a *Gmmips* gene isolated from immature soybean seeds. When crude protein from Arabidopsis siliques of all developmental stages was analyzed, low levels of *At*MIPS were detected (Figure 2.9). However, *Gmmips* transcript in seeds (Hegeman et al., unpublished data) and *Osmips* transcript in embryos (Yoshida et al., 1999) accumulated to high levels at specific developmental stages. Analyzing siliques pooled over many stages may have made detection more difficult. Therefore, siliques were separated by size to differentiate developmental stages. Siliques used for this analysis were separated into two groups (1) mature siliques 13 mm in length or greater and (2) immature siliques less than 5 mm in length. Crude total protein extracts from each group, mature and immature, were separated by SDS-PAGE and blotted using the affinity purified

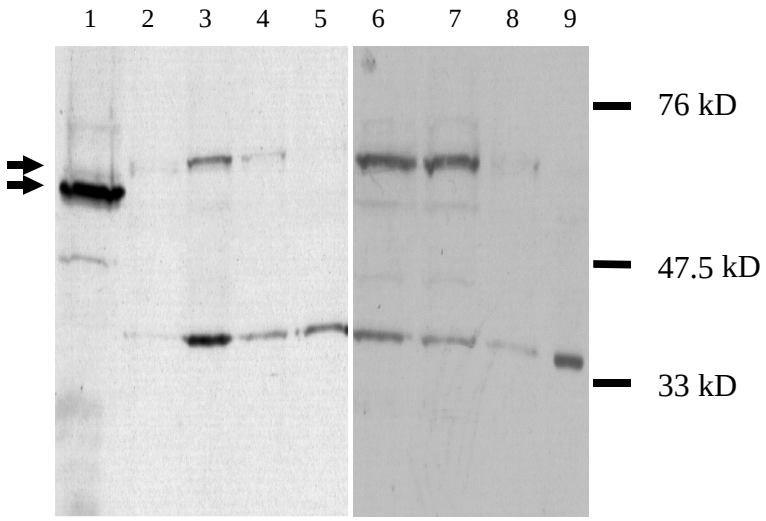

Figure 2.9 Protein blot analysis of *At*MIPS. Crude total protein extracts were separated by SDS-PAGE and transferred to nitrocellulose using the wet tank transfer technique. Proteins were immuno-detected with the affinity purified anti-*Gm*MIPS antiserum. The top black arrow denotes *At*MIPS and the bottom arrow indicates *Gm*MIPS. (1) Soybean (2) Siliques (3) Seedlings Aged 1 Month (4) Seedlings Aged 2 Weeks (5) Cauline Leaves (6) Opened Flowers (7) Immature Flowers (8) Rosette Leaves (9) Bolts.

anti-*Gm*MIPS antiserum (Figure 2.10). Immature Arabidopsis siliques accumulated higher levels of *At*MIPS than mature siliques (lanes are have approximately 25 μg of crude protein). Also, more than one protein may be detected in the immature lane.

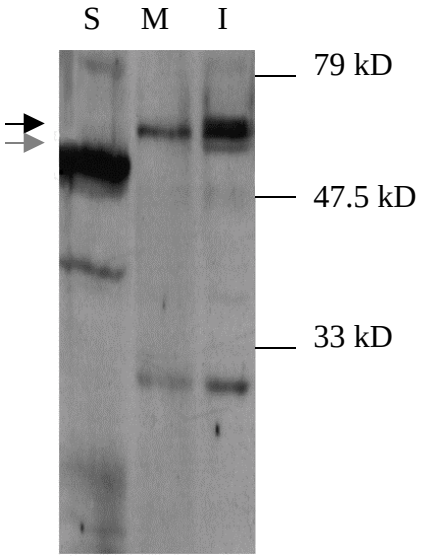

Figure 2.10 *At*MIPS expression in mature and immature Arabidopsis siliques. Crude total protein extracts from immature soybean seeds (S) (positive plant control), mature siliques (M) (> 13mm in length), and immature siliques (I) (< 5mm in length) were separated on SDS-PAGE, transferred to nitrocellulose and incubated with 1:50,000 affinity purified anti-*Gm*MIPS antiserum. The black arrow indicates the *At*MIPS and the gray arrow indicates *Gm*MIPS (apparent molecular mass 64 kD). Note that there may be one or more isoforms of *At*MIPS between 65 and 66 kD.

DISCUSSION

MIPS IS A HIGHLY CONSERVED PROTEIN

An anti-*Gm*MIPS antiserum has been produced to detect MIPS protein accumulation patterns in both Arabidopsis and soybean. Since an antibody recognizes a minimum epitope of 8 residues, I hypothesized that an antiserum produced against the *Gm*MIPS protein would cross react with the *At*MIPS isoforms. Phylogenetic analysis of the predicted amino acid sequences from many plant species (Figure 2.1) indicated that these proteins separate to individual branches; however, the percentage divergence between these branches is not greater than 8%. Predicted amino acid sequence alignment demonstrated that *At*MIPS-1, -2 and *Gm*MIPS proteins were found in the dicot branch of this analysis; and *At*MIPS-1 and -2 were found to be 86.7% and 89.9% identical to *Gm*MIPS, respectively. Additionally, MIPS antisera have been reported that cross-react with MIPS proteins more divergent than *At*MIPS-1 (Johnson and Sussex, 1994), *At*MIPS-2 (Johnson and Burk, 1995) and *Gm*MIPS (Hegeman et al., unpublished). *Sc*MIPS was found to cross react with *Pv*MIPS (Johnson and Wang, 1996) and *At*MIPS (Johnson and Sussex, 1995) and anti-*Eg*MIPS antiserum was found to cross react with cyanobacteria, rice and the mung bean (RayChaudhuri et al., 1998). Interestingly, the anti-*Gm*MIPS antiserum did not cross react with the *Sp*MIPS protein under our blotting conditions (data not shown).

OVEREXPRESSION AND PURIFICATION OF THE RECOMBINANT PROTEIN

The antigen used to produce the anti-*Gm*MIPS antiserum was a recombinant *Gm*MIPS protein overexpressed in a bacterial system. The overexpressed gene was a portion of the cDNA from an immature soybean seed MIPS. The protein was confirmed to be HISMIPS throughout the extraction and purification process as indicated by the Ni^{2+}-AP-conjugate precipitate formation. The antigen overexpression and purification procedure required many optimization steps due to the insoluble nature of the protein. When proteins are overexpressed in a prokaryotic system such as this, the target protein is produced at levels much higher than may be tolerated by the bacterium. Therefore,

bacteria can compartmentalize the protein into inclusion bodies, thus rendering the protein non-toxic and insoluble. Chaotrophic agents, such as urea, can unfold proteins in the inclusion bodies rendering them soluble and facilitating easy purification. In this study, I found that the recombinant protein was not soluble and most likely contained in inclusion bodies. In order to extract large amounts of the HISMIPS protein denaturing conditions were used.

HISMIPS protein purification was simplified due to the 6X-histidine tag. When using denaturing conditions for protein extraction the major factor affecting the release of the 6X-histidine tag from the Ni^{2+}-NTA agarose beads was pH. Lysate was bound under alkaline conditions and released under acidic conditions. Much of the chemistry related to the release of the recombinant protein is based upon the pKa (6.0) of the histidine residue. Histidine is protonated under physiological conditions, pH 7.0. Protein binding occurs at pH 8.0 when the histidine tag is deprotonated. After binding, the beads are washed in a solution of pH 6.3, which is slightly more acidic, causing non-specific proteins, or those with a few histidine residues, to disassociate. Finally, the histidine tagged protein is eluted from the column with buffer pH 4.5. Acidic buffer causes the histidine to gain a proton and disassociate from the column.

In an effort to elute the HISMIPS protein with the highest possible yield and purity, imidazole was also added to the wash and elution buffers. Imidazole is a competitor for the Ni^{2+} sites and at high concentrations (~250 mM) causes disassociation of the histidine tag.

CHARACTERIZATION AND PURIFICATION OF THE ANTI-GmMIPS ANTISERUM

The anti-*Gm*MIPS antiserum was produced and found to cross react with HISMIPS, *Gm*MIPS and *At*MIPS. The crude anti-*Gm*MIPS antiserum coupled with the semi-dry transfer technique, detected a 76 kD protein in the total bacterial protein extracts that contained the HISMIPS protein. *Gm*MIPS was also detected using this technique and was calculated to have an apparent molecular mass (64 kD) which is similar to, yet

somewhat higher, than the calculated molecular mass (56 kD) based on the predicted amino acid sequence.

*At*MIPS was undetectable until the transfer method was optimized. Semi-dry transfer is ideal for lower molecular mass proteins, while a wet tank transfer method was better for proteins of a higher molecular mass. Since *At*MIPS-1 and -2 have predicted molecular masses of 56.5 and 56.2 kD, wet tank transfer proved to be more efficient. When the transfer technique was altered, a protein of 66 kD was detected, and also a second protein at 65 kD in immature siliques. The apparent molecular mass for *At*MIPS-1 was similar to that found by Johnson and Sussex (1993) using anti-*Sc*MIPS antiserum.

Although the wet tank transfer coupled with the crude antiserum allowed for the detection of the *At*MIPS protein, the background was high. This made it difficult to differentiate *At*MIPS isoforms from background bands. Therefore it was necessary to affinity purify the antiserum. First, a nitrocellulose strip purification technique was employed. This technique enhanced detection of a 34 kD protein with unknown identity (discussed below), but not the *At*MIPS and *Gm*MIPS proteins. Affinity purification by subtractive column enhanced the detection of *At*MIPS protein. This procedure also removed many of the background bands associated with the wet tank transfer.

*At*MIPS, *Gm*MIPS and HISMIPS all migrate slower than would be expected as based on their predicted molecular masses. *At*MIPS-1 migrates at 66 kD; *Gm*MIPS migrates at 64 kD, and HISMIPS migrates at 76 kD. However, the predicted molecular masses are based solely on the amino acid sequence and do not include any post-translational modifications that would change the molecular masses. In addition, analysis of immature Arabidopsis siliques suggests a second *At*MIPS isoform that migrates at 65 kD. Further analysis of the native *At*MIPS protein needs to be completed to better understand the true molecular mass of the proteins.

MIPS AND THE SPATIAL AND TEMPORAL PRODUCTION OF INOSITOL

Compounds containing inositol are abundant in plant cells (for review see Loewus and Loewus, 1984). The single route for *de novo* inositol biosynthesis in plants is dependent on MIPS. Therefore, the regulation of MIPS may be highly complex and developmentally regulated. My results indicate *At*MIPS accumulates preferentially in Arabidopsis tissues undergoing changes such embryo, pollen, and seed development.

Keller et al. (1999) found *St*MIPs were light/dark regulated. *At*MIPS protein accumulates at lower levels in etiolated seedlings versus light grown seedlings. The light dark regulation of this protein may also provide insight into the possible identity of the 34 kD protein, since this protein is also light dark regulated

IDENTITY OF THE 34 KD PROTEIN

The 34 kD protein detected using both the nitrocellulose strip purified and the affinity purified antiserum was also detected by Johnson and Wang, (1996) in Arabidopsis using the anti-*Sc*MIPS antiserum. The anti-*Sc*MIPS antiserum was raised against *Sc*MIPS purified by traditional protein purification means and not an epitope tagged protein. Johnson and Wang (1996) localized this protein to the chloroplastic stroma. This is an interesting finding in Arabidopsis because a chloroplastic isoform of this particular size has not be indicated since by other researchers. In fact, most researchers detect MIPS proteins between 60 and 67 kD (Nelson et al., 1998; RayChaudhuri et al., 1997). Chloroplastic MIPS have been isolated and detected in rice and mung bean but have much larger molecular masses than the 33 kD (RayChaudhuri et al., 1997). Nevertheless, the smaller mass of the chloroplastic Arabidopsis protein (Johnson and Wang, 1996) is not entirely surprising in light of the results presented by RayChaudhuri et al. (1997) since chloroplastic proteins tend to be smaller than cytosolic proteins. Further experiments need to be completed to determine if the 34 kD protein is *At*MIPS. These experiments might include analyzing a protein blot of isolated chloroplasts.

DIFFERENTIATION OF AtMIPS ISOFORMS USING ANTI-GmMIPS ANTISERUM

The anti-*Gm*MIPS antiserum described was raised against a plant fusion protein and found to cross-react with MIPS proteins from both a model system and a crop species. Previous polyclonal antibodies used to detect plant MIPS proteins were raised against either non-plant species, *Sc*MIPS (Johnson and Henry, 1989) and *Eg*MIPS (RayChaudhuri et al., 1997), or the halophytic ice plant *Mc*MIPS (Nelson et al., 1998). The amino acid sequences are not as highly conserved between non-plant species and plant species, therefore, the anti-*Gm*MIPS antiserum may provide a more sensitive tool for analyzing isoforms of plant MIPS proteins. The anti-*Sc*MIPS antiserum cross-reacts with *At*MIPS and *Pv*MIPS (Johnson and Wang, 1996), however, the percent similarity between the plant and yeast MIPS proteins is 61.5%, whereas the plant MIPS proteins 85% to 92% similar. To date, the anti-*Sc*MIPS antiserum raised against *Sc*MIPS has been found to detect only one isoform of *At*MIPS (64 kD). Two *At*MIPS genes have been established reverifying two *At*MIPS isoforms exist in Arabidopsis (Johnson and Sussex, 1994). The second isoform, *At*MIPS-2, has found to be catalytically active *in vitro* (Johnson and Burk, 1995). The anti-*Eg*MIPS antiserum was found to cross react with both cytosolic and chloroplastic isoforms of *Os*MIPS and *Vr*MIPS, but to varying degrees (RayChaudhuri et al., 1997). Although anti-*Mc*MIPS antiserum has been used to detect *Mc*MIPS, this antiserum has not been used to detect MIPS from other organisms (Nelson et al., 1998). This may be a valuable tool for detecting MIPS isoforms since (1) the antiserum produced in this study was raised against a plant MIPS that has a higher amino acid sequence similarity than non-plant MIPS and (2) preliminary data using the affinity purified anti-*Gm*MIPS antiserum supports the detection two *At*MIPS isoforms near 66 kD (Holbrook and Gillaspy, unpublished data). In tomato, an anti-*Le*IMP-1 antiserum was raised against a recombinant *Le*IMP-1 and was found to be a useful tool for detecting multiple isoforms of the *Leimp* gene family. The antiserum was raised against one isoform and was found to cross react with the other two *Le*IMPs.

CONCLUSION

I postulate that there are two isoforms of *At*MIPS and that these isoforms are developmentally regulated. The anti-*Gm*MIPS antiserum detects *At*MIPS protein that is spatially and temporally regulated in Arabidopsis tissues. However, further protein blots are needed to elucidate the expression patterns of the two *At*MIPS isoforms. The ability to detect MIPS protein accumulation will provide the means to dissect the regulation of MIPS in Arabidopsis, crop species and other related economically important plant species.

PART III: REGULATING INOSITOL BIOSYNTHESIS IN PLANTS: *MYO*-INOSITOL MONOPHOSPHATASE

INTRODUCTION

Inositol is important for normal plant growth and development. It is involved in signal transduction, phytic acid biosynthesis, auxin storage and transport, cell wall biosynthesis and the production of salt tolerance related molecules (for review see Loewus and Murthy, 2000). There are two routes for the production of inositol. These are (1) the *de novo* inositol biosynthesis pathway and (2) the scavenging of inositol phosphates. The *de novo* inositol biosynthesis pathway converts the common metabolite, glucose-6-phosphate to 1D-inositol-3-phosphate, which is further dephosphorylated through the use of the enzyme IMP. Inositol is also recycled through the sequential breakdown of the second messenger, IP_3 and the phosphorous storage molecule, IP_6. However, regardless of the production route, IMP is involved in the last step of inositol production by catalyzing the removal of a single phosphate group from an inositol phosphate substrate to produce inositol.

IMP has only been studied in a few plant species. A detailed picture of IMP, in particular in relation to functionality in plants, has been provided from studies on *Lycoperscicon esculentum* (tomato) (Gillaspy et al., 1995). In tomato, *Le*IMP is encoded by a multigene family consisting of *Leimp* -1, -2 and -3. These genes encode three spatially and temporally regulated proteins with molecular masses of 30, 29 and 28 kD, respectively (Gillaspy et al., 1995). An anti-*Le*IMP-1 antiserum was produced and affinity purified that cross-reacted with all three isoforms. Protein blot analysis of different tomato developmental stages indicates *Le*IMP proteins may accumulate in callus, light grown seedlings, roots, leaves, young fruit, 1-cm diameter fruit and mature green fruit. *Le*IMP-2 protein accumulates to a higher degree than *Le*IMP-1 or -3, especially in callus, young fruit and mature green fruit.

RNAse protection assays indicated that *Leimp*-1 transcript was most highly expressed in flowers, young and mature green fruit, light grown seedlings and callus; *Leimp*-3 accumulation was found to be highest in seedlings, roots and young fruit (Gillaspy et al., 1995). However, *Leimp*-2 transcript was 10-fold less abundant than

Leimp-1 or -3 (Gillaspy et al., 1995). This finding, coupled with the abundance of the *Le*IMP-2 protein, indicates that *Le*IMP-2 may be expressed at high levels in specific cell types. This result also suggests post-transciptional regulation of *Le*IMP-2.

In this part of my thesis, I analyzed a previously isolated genomic clone of *Leimp*-2 and *Leimp*-2 promoter::*uid*A transgenic plants. Cis-acting regulatory elements found within the 5' UTR include the TATA box and light and cold responsive elements. Interestingly, the analysis of *Leimp*-2 promoter::*uid*A transgenic plants indicated that the *Leimp*-2 promoter is expressed in specific cell types and may be involved in abaxial signaling.

MATERIALS AND METHODS

PROMOTER ANALYSIS

The promoter sequence of *Leimp*-2 was previously cloned and sequenced by J. Keddie (University of California at Berkeley). The genomic clone was analyzed using tools available on the web site Plant Cis-Acting Regulatory Element (Plant C.A.R.E.) (Rombauts et al., 1999).

PLANT MATERIALS

Plant material consisted of *Lycopersicon esculentum* cv. Ailsa Craig wild type, and four independent lines of *Leimp*-2 promoter::*uid*A transgenic plants in the Ailsa Craig background. For germination, seeds were surface sterilized for 10 minutes using 30% Clorox and rinsed with sterile water. Seeds were germinated on 0.5 X Murashige and Skoog Basal Salt Mixture (MS Salts) (Sigma) in Magenta boxes for 10, 13, 15 and 20 days. Plants were grown at 22^{o}C under continuous light in a growth chamber (Percival Scientific). Media for transgenic plants contained 50 μg/ml of kanamyacin. Seedlings at different ages were used to determine age-related patterns. The shoot apex, branch points, cotyledons, true leaves and hypocotyls of control and the transgenic plants were dissected using a sterilized double-edged razor blade.

GUS ASSAYS

The GUS assay (Jefferson, 1987) involves infiltrating a chromogenic substrate into plant tissue which produces a blue precipitate when it is hydrolyzed. Sample tissues were immersed in GUS assay solution (0.025 μM ferrocyanide, 0.025 μM ferrous cyanide, 0.1 mM sodium phosphate buffer pH 7.0, 0.01% Triton X-100, 0.5 μg/ml 5-bromo-4-chloro-3-indoyl-β-D-glucuronic acid), vacuum infiltrated for 30 minutes and incubated at 37^{o}C overnight. After incubation, the assay solution was replaced by formalin-acid-alcohol (FAA: 50% (v/v) ethanol, 10% (v/v) 37% formaldehyde, 5% (v/v) glacial acetic acid) to preserve the tissue morphology. Tissues were stored at 4^{o}C.

MACROSCOPIC AND MICROSCOPIC ANALYSIS

Whole tissue samples were examined using a stereomicroscope (Stemi SVII Apo, Ziess). Samples were transferred to sterile water and viewed on a glass slide at a magnification of 6.0 X and 10.0 X. Results were recorded using a digital camera (3CCD Camera, MIT) and prepared for publication using Adobe PhotoShop 5.0.

Slides were viewed using a Ziess Axioscope 2 compound microscope. Darkfield microscopy was used to visualize the cells containing the GUS precipitate. Under darkfield conditions the precipitate formed by the GUS assay appears bright pink and cell walls are light gray. Images were recorded using a Spot Digital Camera (SPOT model 1.4.0. Diagnostic Instruments, Inc.) and analyzed using Adobe PhotoShop 5.0.

HISTOLOGY

Tomato seedling tissue was fixed in FAA, embedded in paraffin, cut into 10 μm sections and viewed using darkfield microscopy (Ruzin, 1996). Fixed samples were dehydrated in increasing solutions of ethanol (50%, 60%, 70%, 80%, 95%, and 100%) at 30-minute intervals. The organic solvent substitute for xylene, Hemo-De (Fisherbrand), was used for transitioning samples between ethanol and paraffin. Samples were transferred to a series of Hemo-De/100% ethanol solutions (7:1, 3:1, 1:1, 1:3, 1:7) and two changes of 100% Hemo-De at 30 minute intervals. Samples were infiltrated with melted paraffin, (Tissue Prep 2, Fisher Scientific) which was added to a final concentration of 50% at 56^{o}C over one day. Wax infiltrated samples were positioned for correct orientation and embedded in small metal dishes. Samples were sectioned with a microtome (Microm HM 330) into 10 μm thick ribbons and affixed to slides (Single Frosted, Corning) by incubating overnight at 37^{o}C. Fixed mounted sections were de-paraffinized in decreasing solutions of Hemo-De and preserved under a 24 mm X 50 mm cover-slip (Corning) using Permount (Fisherbrand).

RESULTS

ISOLATION AND ANALYSIS OF THE Leimp-2 GENE

A 3.3 kb fragment encompassing the coding region of *Leimp*-2 and 1,908 bp of the 5' untranslated regions (UTR) was isolated from a tomato genomic library and sequenced (J. Keddie, University of California at Berkeley). This *Leimp*-2 clone was used to probe a tomato genomic DNA blot to confirm the presence and copy number of *Leimp*-2 (Figure 3.1) (J. Keddie, University of California at Berkeley). The results indicated that *Leimp*-2 is a single copy gene and contains an internal *Hind*III site. These data were supported by a restriction endonuclease site search of the *Leimp*-2 genomic clone using the computer software program MapDraw (Lasergene, DNAStar).

Two open reading frames (ORFs) were identified within the 3.3 kb fragment (Figure 3.1). The first ORF corresponds to the 3' end of a tomato calmodulin-like gene, as determined from a BLAST search using the predicted protein sequence. The second ORF was identical to the previously identified *Leimp*-2 cDNA clone isolated from a young tomato fruit cDNA expression library (Gillaspy et al., 1995; Accession number in Table 1.1). Interestingly, the second ORF is intron-less. In the *Leimp* multigene family, this phenomenon is unique to *Leimp*-2, as both *Leimp*-1 and *Leimp*-3 genes contain introns as indicated by sequencing efforts and PCR amplification of tomato genomic DNA, respectively (data not shown). Specifically, the *Leimp*-1 gene has been shown to contain 12 exons separated by 11 introns while *Leimp*-3 sequencing is still in progress.

The 5' and 3' UTRs of *Leimp*-2 were analyzed using the internet sequence analysis tool Plant Cis-Acting Regulatory Elements (Plant C.A.R.E.) (Rombauts et al., 1999). Putative regulatory sites are indicated in Figure 3.2A. Three putative light regulatory elements were identified: Regions I, III and IV can be found at bases - 684 to - 677, - 454 to - 466 and - 413 to - 420 respectively. Region I and III (tttcaaa) are elements previously described as carboxy-lyase (Kuhlemeier, 1988) and ribulose bisphosphate genes (for review see Manzara and Gruissem, 1988).

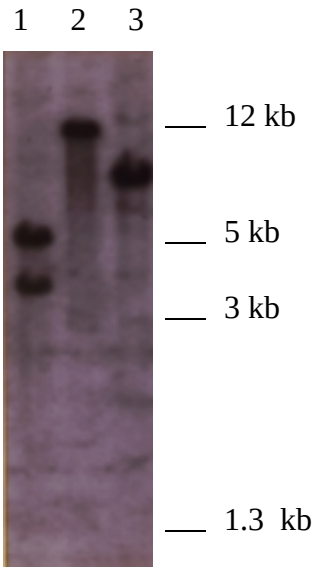

Figure 3.1 Southern blot of tomato DNA with *Leimp*-2 probe. Tomato seedling genomic DNA was digested using *Hind*III (1), *Eco*RI (2) or *Bam*HI (3), separated on an agarose gel and visualized with ethidum bromide. After the DNA was transferred to a nylon membrane, the blot was probed with *Leimp*-2 probe. These results indicate *Leimp*-2 present in the genome in single copy with an internal *Hind*III site.

A

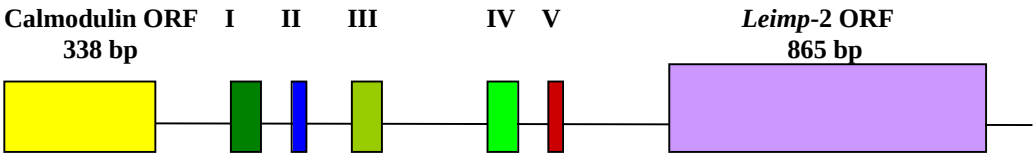

B

```
GATCCATAGGAGAACATATGTCACATGAGGATGCTCAAGAAATCGTAGATGAACTCGATAGGGATGGTGATA –1483

ATTTCATAGATTTTGATGATTTTAAGAAGTTGTTGATGCAAAAAGAAGGAGGTAGTGAAGAGGATGAATCGT –1411

TAAAGTAAGCATTTGAAATGTATGAAGTTGAAAAAGGTTGTGGTCGGATTACACCTAAAAGTTTACAGAGAG –1339

TTTTGAGTCGTTTAGGGGATTCAAAATCTTACGACGAATGTGTTACTATGATCAAAGTATATGACATTGATG –1267

GTAATGGGGAACTTGATTATCATGAATTTCGCCAAATGATGACGACTTAAtcagaaaaaaataaataaaatg –1195

Aaagtagaacaaatatatacaaaaataaataagagcatgatattgaatggctgagacaacaaaaagtaaaga –1123

aaatctcaggactcggcttgtctataattaattgttcttcttagtattgtagttttgtaacatattttgttt –1051

taaatccttcaaaatattatttttggatacatctattgatgataaattagaattattctttttgtggttctt –979

gttcttgtgcgatgtatcagcagcacttttttctagcgatagaacaacaagatttaatttattgggtagattt –907

cataaatagctagagtttgaaatatatgagtctccttaacagtagttgaactaaagttttcttactttcttt –828

gtatgtctcgctgaaagtttaatttcttatacaaattagactcttcacttaattcatcaggcagtaattgcg –756

tcttaaaaggtcaataaactataggaaattatgtaacaaagtaattaaattttatttttatatcaataaaatc –684

actcaacttaaatatatacatttttccatttaaacaaattttagatgacaatttaaattatttttttatgtca –612
                                                                    I
tataattataaatatgaactccacagataaataaagttataaaatctattaa tttcaaa agtaacttaaatc –540
                 II
tcaactctatgaaa ccgaa aagggacggtaaattagaccccataatacacaggatgcttggcatcaattagc –468
                                        III
cacatgaataattaggatcagccactcgatatata agaaacaa caaagtacgaaaatacagatgccaagaaa –396

gttagcaaaaatctgagtaattcattttctctgaacaagacgtcgtttccgatcgaatttgtttgaaatttg –324
            IV
ggcgatacgt tttcaaa ctgatggcatagagctagagaggggggaaaaaaaatcggagtagagtccatgatta –252

tacgacttgaaaataatttaatttgtcatttaaaaattattttatcgataaatgtaaataatagatttttta –180

agataaaaatttaaagttgagtgctcttattaataaaaaacaaaatttagataatttctcatagttataaac –108

atgtaataaaatcctgttagaatagaaataagaaaaagaagggtatataaaattctacttgaaaaagcagta –36
  V                                  +1
g tatata aaatccaactttgaaaaggattagtatatataacccaacctgaaaaaggatactagagtgtctat 35

aagtaggaattatgtaaagacacaattcaatagtaatatttttgttaggcaattcaatagtaaattaaaaca 107

gATGGAAGAGTTTGTTGAGTGTGCAATTGAAGCAGCTAAGAAAGCCGGAGAGATAATTCGTCATGGATTCTA 179

CAAGAGTAAGCATATTGAGCACAAAGGAGTTGTTGATTTAGTGACAGAGACTGATAAGGCATGTGAAGTTTT 251

AATTTTTAATCATCTGAAGCAATGTTTTCCTAGTCATAAGTTCATTGGTGAAGAAACAACTGCTGCTGCTTC 323

TGGAAATTTTGAGTCTACTGATGAACCAACTTGGATAGTTGATCCACTTGATGGAACTACTAACTTTGTGCA 395
```

```
TGGCTTCCCTTTTGTTTGTGTATCTATCGGTCTCACAATTGAAAAGAAACCAGTGGTTGGTGTTGTTTACAA 467

CCCAATCATCGACGAGCTTTTCACTGCAATCTATGGGAGAGGTGCTTTTCTTAATGGGAAGTCCATCAGAGT 539

ATCTTCAGAGTCTCAACTTGTAAAAGCTCTTGTTGCTACAGAGGTTGGAACAAACAGGGATAAGGCAATTGT 611

AGATGCTACTACAGGAAGAATTAATAGAGTGATTTTCAAGGTTAGGTCCCTCAGGATGTCTGGTTCTTGTGC 683

ATTAAATCTATGTGGAGTGGCGTGTGGAAGGCTTGATCTCTTCTATGAAATTGAATTTGGTGGTCCGTGGGA 755

GTGCGCAGCTGGTGCTCTCATAGTCATAGAAGCTGGAGGACTCGTTCTTGATCCATCTGGTTCCGAATTTGA 827

CCTAACAGCTCGACGTGTAGCTGCTACAAACGCTCATCTCAAGGACGCTTTTATCAACGCCTTGAATGAATC 899

AGAATGAgaatcatactttcatacacaataggaataggaagaagaatgcaataattatttgtactgtgaata 971

Ttgttatgcatagattatttactttagggatctttgttgttactggaaaaaataaataaggaaaaatgtatt 1043

Cagtagaaattgatccctgaacctcccagtaaaaaagttttgatttctatatattgttcttgttcctattcc 1115

tattctaacactattaagtgtgttggtaaacaccactcacaagtatcacctaattgaagctt           1187
```

Figure 3.2 Genomic DNA sequence of *Leimp*-2 does not contain introns. *Leimp*-2 was obtained by screening a tomato genomic library, and the sequence was analyzed using the computer program Plant Cis-Acting Regulatory Elements (CARE) and Lasergene. **(A)** Genomic structure. Analysis of the 5' untranslated regions (UTR) identified five regions of cis-acting regulatory sequences. Putative regulatory elements are as follows: Regions I, III, IV: light responsive elements, Region II: cold responsive element and Region V: TATA box. **(B)** Genomic sequence. The 5' and 3' UTRs are denoted with lowercase letters and the putative open reading frame (ORF) is denoted with uppercase letters. The putative ORF encodes 266 amino acids and has been found to produce a 29 kD protein (Gillaspy et al., 1995).

Region IV (agaaacaa) is an element involved in the regulation of the subunit A gene of glyceraldehyde 3-phosphate dehydrogenease (for review see Terzaghi and Cashmore, 1995). As light regulation of both *Leimp*-2 mRNA and protein has been previously characterized (Gillaspy et al., 1995), it is likely that one or more of these elements functions in light regulation of transcription.

Region II (ccgaaa) may be involved in cold responsiveness. This element can be found at bases - 527 to - 522. The region is identical to the element previously described as a low temperature responsive element in *Hordeum vulgare* (Dunn et al., 1998).

Region V (-30 to -24) corresponds to the consensus TATA box motif that controls initiation by RNA polymerase II. The putative start site of transcription is located downstream from the TATA box motif at +1. The putative start site of translation is located at +108 bp downstream of the putative start site of transcription.

The 3'UTR was also sequenced. Although 3'UTRs sometimes exhibit regulatory effects, no elements were detected using Plant C.A.R.E. for this region in *Leimp*-2.

Leimp-2 IS DEVELOPMENTALLY REGULATED IN TOMATO SEEDLINGS

To characterize the expression of the *Leimp*-2 gene at the tissue and cellular level, a 2.1kb *Cla*I fragment of the *Leimp*-2 promoter was fused to the *uid*A gene coding region and transferred into tomato plants by *Agrobacterium tumefaciens*-mediated transformation (An et al., 1986). The bacterial *uid*A gene encodes the β-glucuronidase (GUS) enzyme that is easily assayed in plant tissues to yield information on the expression pattern of the promoter used to drive expression. Initial *Leimp*-2 promoter::*uid*A transformants were selected and characterized for presence of the transgene insert and selfed to produce T_2 transgenic *Leimp*-2 promoter::*uid*A plants (performed by J. Keddie, University of California at Berkeley).

For my studies, seed from homozygous T_2 *Leimp*-2 promoter::*uid*A plants were germinated and grown for 10, 13, 15 and 20 days in Magenta boxes. The GUS expression assay was completed using four independent lines of transgenic *Leimp*-2 promoter::*uid*A seedlings. Each line showed the same expression pattern in tissues of the same developmental stage, as opposed to control plants that did not indicate GUS precipitate (Figure 3.3B). *Leimp*-2 promoter::*uid*A seedlings showed spatial regulation of *Leimp*-2 as evidenced by bright blue staining in the shoot apex, the internode or branch point, and the base of leaflets (Figure 3.3C). The most intense deposition of precipitate was found below the shoot apex and extended on the abaxial side of the compound leaf stem above the shoot apex. Furthermore, *Leimp*-2 is expressed in two abaxial "lines" which run parallel to each other from the internode to the first set of fully expanded leaflets. This pattern is only evident in the fully expanded compound leaf nearest the shoot apex and not in other older (fully expanded leaves 3 or more leaves below the shoot apex) or younger leaves (not fully expanded immature leaves nearest the shoot apex). GUS precipitate patterns were identical in tissues at the same developmental stage regardless of the seedling age.

To determine which cell layers in the stem and apical meristem express *Leimp*-2, *Leimp*-2 promoter::*uid*A tissues were stained for GUS activity, preserved by chemical fixation, and embedded in paraffin. In sections of *Leimp*-2 promoter::*uid*A tissues, *Leimp*-2 expression was observed in specific cell types. These included the epidermis, the cortex on the abaxial leaf surface and the tunica of the apical meristem (Figure 3.3 G and H). These results indicated that only a few cell types of young seedlings express *Leimp*-2, and are in agreement with our previous data which indicated that *Leimp*-2 steady-state mRNA levels in seedlings are very low (Gillaspy et al., 1995). This illustrates the strength of analyzing cellular expression using promoter and reporter gene fusions.

Leimp-2 was most intense at the seedling internodes (Figure 3.2 D, E, and F). Interestingly, GUS staining was most intense at the base of the shoot apex where the leaf

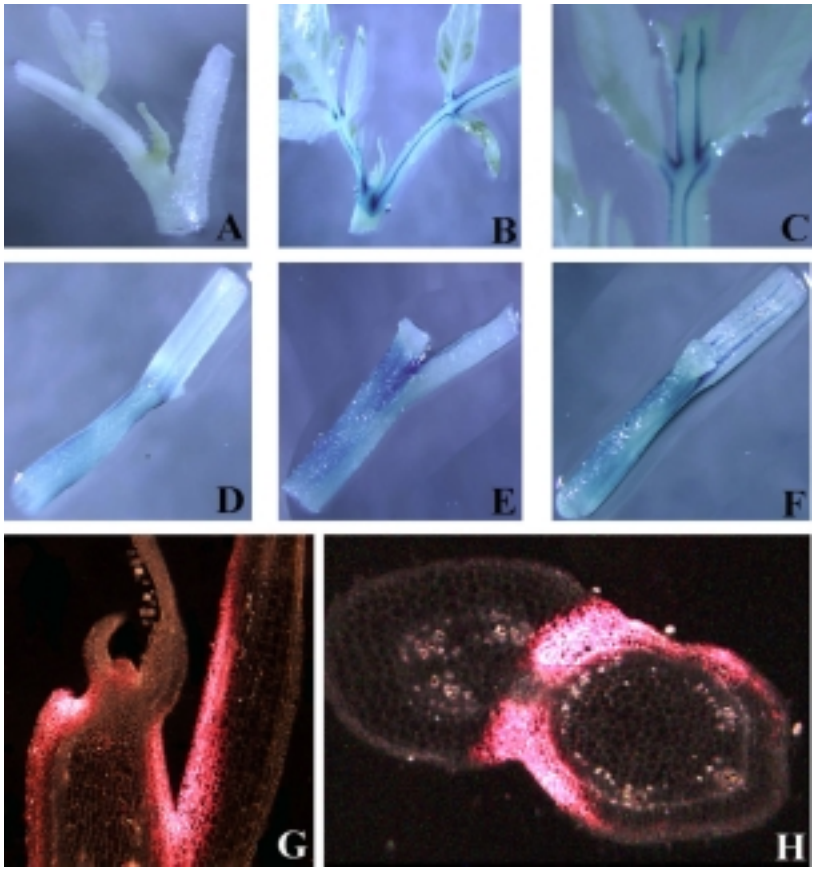

Figure 3.3 Expression patterns of *Leimp*-2. The *Leimp*-2 promoter was fused to the *uid*A reporter gene and transformed into tomato. Transgenic plants were assayed for GUS activity. GUS stain is visualized as a bright blue precipitate using bright field and as a pink color using dark field microscopy. (A) Control seedling shoot apex and compound leaf stem at a magnification of 6X. (B) *Leimp*-2 promoter::*uid*A seedling shoot apex and compound leaf stem at a magnification of 6X (C) *Leimp*-2 promoter::*uid*A seedling leaflets and compound leaf at a magnification of 10X (D) Adaxial internode surface at a magnification of 6X (E) Side surface of internode at a magnification of 6X (F) Abaxial surface of internode at a magnification of 6X (G) Longitudinal section of the shoot apical meristem at a magnification of 100X (H) Transverse section of the base of the shoot apex at a magnification of 200X.

extends beyond the stem of the seedling. Since staining appeared to be most only in specific tissues and cell types, but also in abaxial dependent manner, studies were undertaken to determine if *Leimp*-2 promoter expression is influenced by a gravity stimulus. Five seedlings of each transgenic line and control seedlings were grown vertically with respect to the gravity vector in Magenta boxes, producing growth along the surface of the medium. After fifteen days, these plants were reoriented 90^{o} such that the plant was parallel to the growth chamber shelf. Seedlings were harvested at 1, 2, 4, 8 and 24 hours after the reorientation, and examined for *Leimp*-2 promoter::*uid*A expression. The change in orientation did not alter the *Leimp*-2 staining patterns observed previously (data not shown).

DISCUSSION

THE Leimp-2 GENE IS INTRON-LESS

Features of the *Leimp*-2 genomic clone were assessed, in particular the *Leimp*-2 ORF and the 5'UTR. The *Leimp*-2 ORF is intron-less. Intron-less genes are rare in plants, however intron-less genes have been documented from tomato (Lui et al., 1997) and rice (Hossian et al., 1996). In tomato, a gene that is involved in starvation tolerance is intron-less (Lui et al., 1997) and in rice there is an intron-less gene for pyruvate decarboxylase (Hossian et al., 1996). Many chloroplastic and mitochondrial genes have few or no introns, possibly due to their prokaryotic origins. Also, transposon insertions into the tomato genome may provide the organism with an intron-less copy of one of the *Le*IMPs. However, upon analysis of the 5' and 3' UTR in tomato, no transponson-related elements, such as an inverted repeat, were found.

5' AND 3' UTRS OF LeIMP-2

Cis-acting regulatory regions were found in the 5'UTR of *Le*IMP-2 using the web based sequence analysis tool Plant C.A.R.E. (Rombauts et al., 1999). The regulatory regions could potentially control light and cold responsiveness. The temporal upregulation of *Leimp*s, as indicated by protein blot analyses (Gillaspy et al., 1995), support the discovery of three light regulatory regions in the *Leimp*-2 5'UTR. In 6-day old tomato seedlings little to no *Le*IMP-2 protein expression is found, however, light grown seedlings of the same age accumulate low levels of *Le*IMP-2 protein (Gillaspy et al., 1995). Presumably, the identified light regulated regions in the *Leimp*-2 promoter function to increase transcription of this gene in response to light.

A cold-responsive element was also noted in the Plant C.A.R.E. (Rombauts et al., 1999) analysis of the *Leimp*-2 promoter. Although *Le*IMP-2 protein accumulation has not been studied relative to cold stress, inositol has been found to be associated with cold stress protection (Bohnert et al., 1995). For example, inositol accumulates as phosphoinositides in the barley aleurone cell during cold stress (Robbins et al., 1999).

Phosphoinositides are important components of the cell membrane and are involved in the PI signaling pathway (see literature review).

In addition to the cis-acting regulatory elements, the 5' region of the *Leimp*-2 gene contains a 266 bp (88 amino acids) sequence for part of a calmodulin gene. Calmodulin, a 148 amino acid protein, binds calcium but otherwise has no enzymatic activity (for review see Fosket, 1994). This protein may be activated in conjunction with PI signaling pathway, perhaps when the second messenger IP_3 activates the release of calcium from intracellular stores. The calmodulin-calcium complex activates regulatory subunits of other enzymes such as calcium-calmodulin dependent protein kinases.

Leimp-2 EXPRESSION IS LOCALIZED TO SPECIFIC TISSUE AND CELL TYPES

An intriguing finding was that the GUS expression was observed in tissues where inositol may accumulate, such as at the base of the shoot apex or at the internode between the leaves (Figure 3.3B). This conclusion is similar to that found by Gillaspy et al. (1995) in regard to *Leimp*-1, -2 and -3 protein and transcript accumulation in tomato seedlings. Two ideas were proposed for why these areas may be targeted for *Le*IMP-2 activity. First, rapidly dividing shoot apical meristem and axillary meristems may need pools of inositol for cell wall biosynthesis, phosphate storage, auxin storage and/or to be recycled into the PI signaling pathway. Secondly, these areas may also be resource sinks for the common metabolite glucose-6-phosphate. Tissues with readily available glucose-6-phosphate may express *Le*IMP-2 to convert 1D-inositol-3-phosphate into free inositol. It would be interesting to determine if *Le*MIPS is also expressed in these tissues.

Cell types that expressed *Leimp*-2 promoter::*uid*A included the epidermis and cortex cells. However, not all the epidermal or cortex cells of the stem or shoot apex expressed the protein. Only those cells on the abaxial side of the stem or those that are near the shoot apex exhibited this pattern. This pattern suggests that *Le*IMP-2 is involved in determining the abaxial side of the stem. A role for IMP in regulating dorsal-ventral specification in *Xenopus laevis* has been found in studies using lithium as an inhibitor of

IMP. *X. laevis* embryos became dorsalized when incubated in the presence of lithium chloride (Kao et al., 1986). Thus, ventral differentiation in the frog may require inositol. In plants *Le*IMP-2 may play a similar role in determining the sidedness of the leaf.

PART IV: FUTURE DIRECTIONS

Considering the many roles of inositol in plants, understanding the production of this six-member carbon ring may provide a foundation for future manipulation of inositol metabolism for potential production of plants which can tolerate salt stress, produce less phytic acid and/or provide better nutrition for farm animals. This research has (1) produced anti-*Gm*MIPS antiserum, which has been found to cross-react with Arabidopsis and soybean MIPS, and (2) analyzed the intron-less genomic clone for *Leimp*-2 and found specific expression patterns of *Leimp*-2 in tomato seedlings.

FUTURE DIRECTIONS FOR MIPS

A comprehensive study of *At*MIPS isoforms is currently underway. Most recently, protein blot analysis of Arabidopsis total seedling extracts has detected two isoforms of *At*MIPS that have apparent molecular weights of 65 and 66 kD. Further studies need to be carried out to delineate the spatial and temporal expression patterns of these isoforms.

Additionally, plants that overexpress and repress (through antisense technology) *At*MIPS-1 have been constructed. In these transgenic plants, *At*MIPS-1 is under the control of a constitutive promoter, the Cauliflower Mosaic Virus 35 S promoter. These plants are currently being screened by using the anti-*Gm*MIPS antiserum (Holbrook and Gillaspy, unpublished data). Independent lines of both *At*MIPS-1 overexpressers and antisense *At*MIPS-1 have been isolated. These plants will help to differentiate how each isoform is used in the plant.

The anti-*Gm*MIPS antiserum will also be used for the cellular localization of *At*MIPS in siliques. The cellular localization of *Os*MIPS transcript in rice indicates that temporal and spatial regulation of *Osmips* coincides with globoid production (Yoshida et al., 1999). This study, combined with those in soybean currently being conducted by L. Good and E. Grabau will provide a more complete picture of MIPS regulation in plants.

FUTURE DIRECTIONS FOR IMP

The genomic clone for *Leimp*-1 is being analyzed (Styer et al., in preparation). Preliminary studies indicate that *Leimp*-1 contains 11 introns and 12 exons. Analysis of the 5'UTR has indicated that this isoform also contains light-responsive cis-acting regulatory regions as described in this thesis.

Since we have demonstrated the spatial regulation of *At*MIPS and can distinguish between the *At*MIPS isoforms, it will be interesting to co-localize the *At*IMP isoforms in the same tissues. I predict that *At*IMP may accumulate in many of the same tissues at *At*MIPS.

PART V: REFERENCES

An, G., Watson, B, and Chang, C. (1986) Transformation of tobacco, tomato, potato and *Arabidopsis thaliana* using a binary Ti vector system. Plant Physiology. 81:301-305.

Bandurski, R.S. (1979) Chemistry and physiology of *myo*-inositol esters of indole 3-acetic acid. In: Wells W.W., Eisenberg, F. Jr . Cyclitols and Phosphoinositides. Academic Press, London, New York, 35-54.

Blewitt, M., Matz, E.C., Davy, D.F. and Burr, B. (1999) ESTs from developing cotton fiber. Direct Submission to GenBank. Accession Number: AW187977.

Bohnert, H.J., Nelson, D.E. and Jensen, R.G. (1995) Adaptations to environmental stresses. The Plant Cell. 7:1099-1111.

Bosch, D., Powell,N., and Wright, F. (1998) Investment returns from three sub-surface microirrigation tubing spacings. Journal of Production Agriculture. 11:371-376.

Cosgrove, D. (1980) Inositol phosphates: their chemistry, biochemistry and physiology. New York. Elsevier Scientific Publishing Company.

Cote, G.G. and Crain, R.C. (1993) Biochemistry of phosphoinositides. Annual Review of Plant Physiology. 44:333-356.

Deckert, G., Warren, P.V., Gaasterland, T., Young, W.G., Lenox, A.L., Graham, D.E., Overbeek, R., Snead, M.A., Keller, M., Aujay, M., Huber, R., Feldman, R.A., Short, J.M., Olson, G.J. and Swanson, R.V. (1998) The complete genome of the hyperthermophilic bacterium *Aquifex aeolicus.* Nature. 392:353-358.

Dunn, M., White, A., Vural, S., and Hughes, M. (1998) Identification of promoter elements in a low temperature responsive gene (blt4.9) from barley (*Hordeum vulgare* L.) Plant Molecular Biology. 38:551-564.

Fosket, D. (1994) Plant growth and development: A molecular approach. Academic Press, San Diego. 329-330.

Gillaspy, G.E., Keddie, J.S., Oda, K., and Gruissem, W. (1995) Plant inositol monophosphatase is a lithium-sensitive enzyme encoded by a multigene family. The Plant Cell. 7:2175-2185.

Hashimoto, A., Yamada, S., and Komori, T. (1999) *Myo*-inositol phosphate synthase. Direct Submission to GenBank. Accession Number:AB032073.

Hossain, M., Huq, E., Grover, A., Dennis, E., Peacock, W., and Hodges, T. (1996) Characterization of pyruvate decarboxylase genes from rice. Plant Molecular Biology. 31:761-770.

Hussain, A., Bourgeois, J., Polvi, S., Tsang, E., Keller, W., and Georges, F. (1996) Cloning of a full length cDNA encoding myo-inositol 1-phosphate synthase from *Brassica napus*. Direct Submission to GenBank. Accession Number: U66307.

Hussain, A., Yan, W., Bock, C., Baga, M., Chibar, R., and Georges, F. (1999) cDNA clone for *myo*-inositol 1-phosphate synthase from wheat. Direct Submission to GenBank. Accession Number:U66307.

Ishitani, M., Majumder, A.L., Bornhouser, A., Michalowski, C.B., Jensen, R. and Bohnert, H. (1996) Coordinate transcription induction of *myo*-inositol metabolism during environmental stress. The Plant Journal. 9:537-548.

Jefferson, R. A. (1987) Assaying chimeric genes in plants: The GUS fusion system. Plant Molecular Biology Reports. 5:387-405.

Johnson, M. (1994) The *Arabidopsis thaliana myo*-inositol 1-phosphate synthase (EC 5.5.1.4). Plant Physiology. 105:1023-1024.

Johnson, M. and Burk, D. (1995) Isozyme of 1l-*myo*-inositol phosphate synthase from Arabidopsis. Plant Physiology. 109(2):721.

Johnson, M. and Henry, S. (1989) Biosynthesis of inositol in yeast: primary structure of *myo*-inositol-1-phosphate synthase and functional analysis of its structural gene, the INO1 locus. Journal of Biological Chemistry. 264:1274-1283.

Johnson, M. and Sussex, I. (1994) 1L-myo-inositol 1-phosphate synthase from *Arabidopsis thaliana*. Plant Physiology. 107:613-619.

Johnson, M. and Wang, X. (1996) Differentially expressed forms of 1l-*myo*-inositol-1-phosphate synthase in *Phaseolus vulgaris*. Journal of Biological Chemistry. 271:17215-17218.

Keller, R., Brearley, C., Trethewey, R., and Muller-Rober, B. (1998) Reduced inositol content and altered morphology in transgenic potato plants inhibited for 1D-*myo*-inositol 3-phosphate synthase. The Plant Journal. 16:403-410.

Kao, K., Masiu, R., and Elinson, R. (1986) Respecification of pattern in *Xenopus laevis* embryos: A novel effect of lithium. Nature. 322:371-373.

Kowalczyk, S. and Bandurski, R. (1991) Enzymatic synthesis of 1-O-(indol-3-ylacetyl)-beta-D-glucose: purification of the enzyme from *Zea mays*, and preparation of antibodies to the enzyme. Biochemistry Journal. 279:509-14.

Kuhlemeier, C., Fluhr, R., Green, P.J., and Chua, N. (1988) Localization and conditional redundancy of regulatory elements in rbcS-3A, a pea gene encoding the small

subunit of ribulose-bisphosphate carboxylase. Proceedings of the National Academy of Science. 85:4622-4666.

Laemmli, U. (1970) Cleavage of structural proteins during the assembly of the head of bacteriophage T4. Nature. 227:680-685.

Larson, S. and Raboy, V. (1999) Linkage mapping of maize and barley *myo*-inositol phosphate synthase DNA sequences: Correspondence with a low phytic acid mutation. Theoretical Applied Genetics. 99:27-36.

Loewus, F. (1990) Structure and occurrence of inositols in plants. In: Inositol Metabolism in Plants. D.J. Morre, W.F. Boss and F.A. Loewus Wiley-Liss, Inc., New York, 1-11.

Loewus, F. and Loewus, M.W. (1983) *Myo*-inositol: Its biosynthesis and metabolism. Annual Review of Plant Physiology. 34:137-161.

Loewus, F. and Murthy, P. (2000) *Myo*-inositol metabolism in plants. Plant Science. Elsevier Science. 150:1-19.

Lui, C., Muchhal, U., and Raghothama, K. (1997) Differential expression of TPS11, a phosphate starvation-induced gene in tomato. Plant Molecular Biology. 33:687-874.

Majerus, P.W. (1992) Inositol phosphate biochemistry. Annual Review of Biochemistry. 61:225-250.

Majumder, A., Johnson, M., and Henry, S. (1997) 1L-*myo*-inositol-1-phosphate synthase. Biochimica et Biophysica Acta. 1348:245-256.

Mallin, M., Burkholder, J., McIver, M., Shank, G., Glasgow, H., Touchetter, B. and Springer, B. (1997) Comparative effects of poultry and swine waste lagoon spills on the quality of receiving streamwaters. Journal of Environmental Quality. 26:1622-1631.

Manzara, T., and Gruissem, W. (1988) Organization and expression of the genes encoding ribulose-1,5-bisphosphate carboxylase in higher plants. Photosynthesis Research. 16:117-139.

Michalczuk, L. and Bandurski, R.S. (1980) UDP-Glucose: indoleacetic acid glucosyl transferase and indoleacetyl-glucose: *myo*-inositol indoleactetyl transferase. Biochemica and Biophysica Research Communications. 93:588-592.

Munnik, T., Irvine, R., and Musgrave, A. (1998) Phospholipid signaling in plants. Biochemica Biosphysica Acta. 1389:222-272.

Nelson, D. and Bohnert, H. (1999) Inositol monophosphatase from *Mesembryanthemum crystallinum*. Direct Submission to GenBank. Accession Number: AF037220.

Nelson, D.E., Rammesmayer, G. and Bohnert, H. (1998) Regulation of cell specific inositol metabolism and transport in plant salinity tolerance. The Plant Cell. 10:753-764

Parthasarathy, L., Vadnal, R., Parthasarathy, R., and Shyamala Devi, C. (1994) Biochemical and molecular properties of lithium sensitive *myo*-inositol monophosphatase. Life Sciences. 54:1127-1142.

Perera, I., Heilmann, I., Boss, W. (1999) Transient and sustained increases in inositol 1,4,5-trisphosphate precede the differential growth response in gravistimulated maize pulvini. Proceeding of the National Academy of Science. 96:5838-43.

RayChaudhuri, A., Hait, N.C., Dasgupta, S., Bhaduri, T.J., Deb, R., Majumder, A.L. (1997) L-*myo*-inositol 1-phosphate synthase from plant sources: Characteristics of the chloroplastic and cytosolic enzymes. Plant Physiology. 115:727-736.

Redenbach, M., Ikeda, K., Yamasaki, M., and Kinashi, H. (1998) Cloning and physical mapping of the *Eco*RI fragments of the giant linear plasmid SCP1. Journal of Bacteriology.180: 2796-9.

Robbins, K., Bhuvarahamurthy, N., Pliska-Matyshak, G., and Murthy, P. (1999) The isolation and characterization of right side out plasma membrane vesicles from barley aleurone cells. Lipids. 34:75-82.

Rombauts, S., Dehais, P., Van Montagu, M., and Rouze, R. (1999) Plant CARE, a plant cis- acting regulatory element database. Nucleic Acids Research. 27:295-296.

Ruzin, S. (1996) Plant microtechnique. NSF Center of Plant Developmental Biology. University of California at Berkeley. 4th Edition, 1-147.

Shears, S. (1996) Inositol pentakis- and hexakisphosphate metabolism adds versatility to the actions of inositol polyphosphates: Novel effects on ion channels and protein traffic. Subcelluar Biochemistry. 26:187-226.

Shirmohammadi, A., Yoon, K., and Magette, W. (1997) Water quality in mixed land use watershed–piedmont region in Maryland. Transactions of the American Society of Agricultural Engineers. 40:1563-1572.

Smart, C. and Fleming, A. (1993) A plant gene with homology to D-*myo*-inositol 3-phosphate synthase is rapidly and spatially up-regulated during ABA-induced morphogenic response in *Spirodela polyrrhiza*. The Plant Journal. 4:279-293.

Smith, D.R., Doucette-Stamm, L.A., Deloughery, C., Lee, H.M., Dubois, J., Aldredge, T., Bashirzadeh, R., Blakely, D., Cook, R., Gilbert, K., Harrison, D., Hoang, L., Keagle, P., Lumm, W., Pothier, B., Qiu, D., Spadafora, R., Vicare, R., Wang,Y., Wierzbowski, J., Gibson, R., Jiwani, N., Caruso, A., Bush, D., Safer, H., Patwell, D., Prabhakar, S., McDougall, S., Shimer, G., Goyal, A., Pietrovski, S., Church, G.M., Daniels, C.J., Mao, J., Rice, P., Nolling, J. and Reeve, J.N. (1997) Complete genome sequence of *Methanobacterium Thermoautotrophicum* DeltaH: Functional analysis and comparative genomics. Journal of Bacteriology. 179:7135-7155.

Styer, J., Keddie, J., Grussiem, W., and Gillaspy, G. (*In preparation*) Structure and expression of inositol monophosphatase –1 and –2 genes from tomato.

Terzagi, W., and Cashmore, A. (1995) Photomorphogenesis: Seeing the light in plant development. Current Biology. 5:466-468.

Thompson, L. (1994) Antioxidants and hormone-mediated health benefits of whole grains. Critical Reviews of Food Science and Nutrition. 34:473-493.

Van-Schilfgaarde, J. (1993) Water management strategies for salinity control. Tasks in Vegetative Science. 28:371-377.

York, J., Odom, A., Murphy, R., Ives, E., and Wente, S. (1999) A phospholipase C dependent inositol polyphosphatase kinase pathway required for efficient messenger RNA export. Science. 285:96-100.

Yoshida, K., Wada, T., Koyama, H., Mizobuchi-Fukoka, R. and Naito, S. (1999) Temporal and spatial patterns of accumulation of the transcript of *myo*-inositol-1-phosphate synthase and phytin-containing particles during seed development. Plant Physiology. 119:65-72.

VITAE

Jean Christine Styer is from Montgomery, Pennsylvania. She graduated 6th in her class from Montgomery Area High School. Jean attended Saint Vincent College from 1992-1997 and received her a Bachelor of Arts in Chemistry with an emphasis in Environmental Chemistry in 1996 and a Bachelor of Arts in Biology with emphasis in Plant Ecology in 1997. In 1997 she was the chief coordinator for the 2nd Pennsylvania Natural History Conference as sponsored by Saint Vincent College, the University of Pittsburgh and the Carnegie Museums of Pittsburgh. As an undergraduate she pursued an undergraduate research project with Walter P. Carson, Ph.D., Cynthia Walter, Ph.D., Stephen Horsley, Ph.D which investigated the impact of white-tailed deer in clear-cut forests of northwestern Pennsylvania. During the summer of 1996 she accepted a National Science Foundation Research Experience for Undergradutes Fellowship with Jack C. Schultz, Ph.D. and Bruce A. McPheron, Ph.D. at Pennsylvania State University, University Park, PA. In 1997 she began graduate school in the Department of Biology at Bucknell University, but joined the Biochemistry Department at Virginia Polytechnic Institute and State University in 1998 when her advisor, Glenda Gillaspy, Ph.D., relocated. Jean will join Monsanto Life Sciences at the company's World Headquarters in St. Louis, MO in March 2000 where she will be part of the seed hybrid research team.